

## Supporting Information

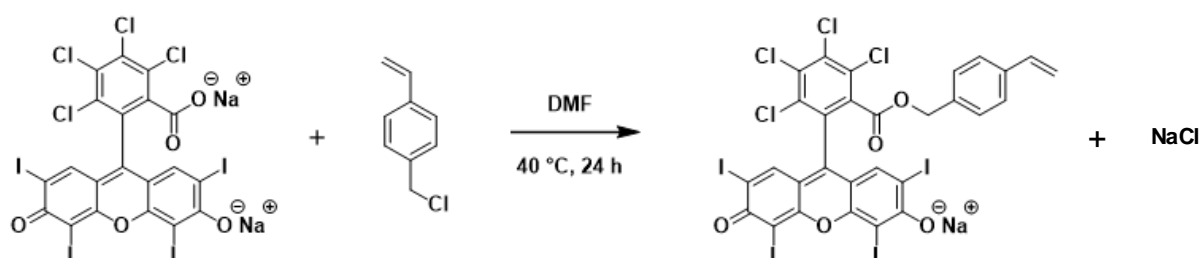
### Photoactive Rose Bengal-based Latex via RAFT Emulsion Polymerization-Induced Self-Assembly

Charlène Boussiron, Mickaël Le Behec, Julia Sabalot, Sylvie Lacombe, Maud Save\*

CNRS, University Pau & Pays Adour, E2S UPPA, Institut des Sciences Analytiques et de Physico-Chimie pour l'Environnement et les Matériaux, IPREM, UMR5254, 64000, PAU, France.

Mail: [maud.save@univ-pau.fr](mailto:maud.save@univ-pau.fr)

#### Synthesis of vinyl benzyl Rose Bengal (VBRB)

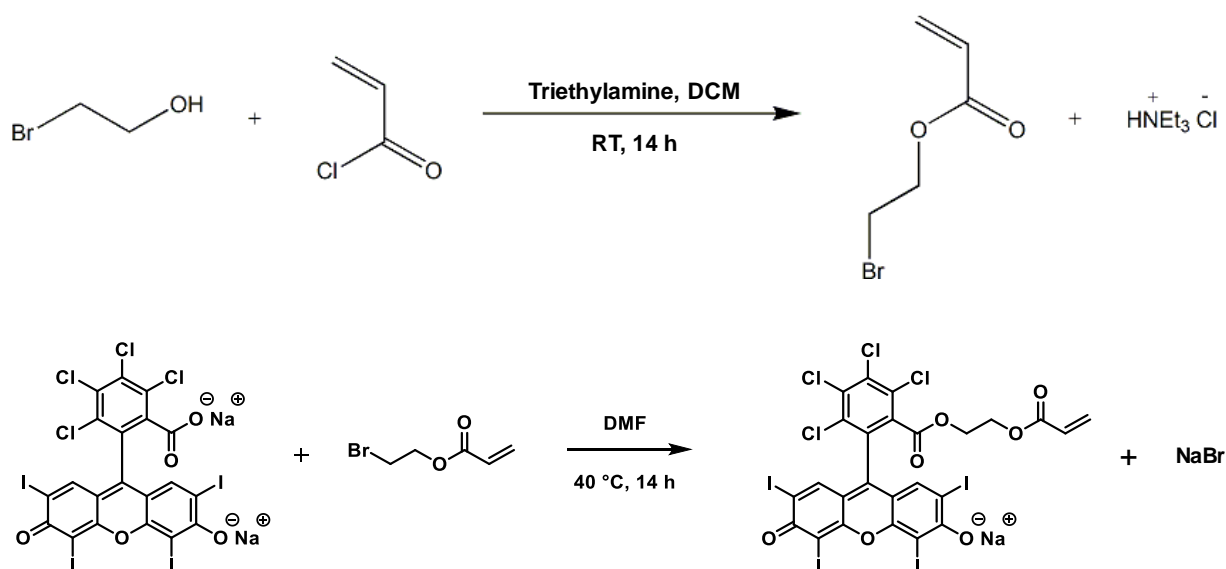


Scheme S 1. Synthesis of vinyl benzyl rose Bengal (VBRB) monomer from Rose Bengal and vinylbenzyl chloride.

Vinyl benzyl chloride (VBC) was reacted with commercial RB in DMF to produce a polymerizable vinyl benzyl Rose Bengal (VBRB) monomer as already described.<sup>1-3</sup> RB (1.831 g, 1.8 mmol) was added to a solution of VBC (0.533 mL, 3.78 mmol) in DMF (40 mL) in a 100 mL round bottom flask dried with a heat gun under argon. The reaction mixture was degassed with a gentle flow of nitrogen for 30 min and was then stirred at 40 °C for 24 h. After cooling down to room temperature, 35 mL of DMF were removed by cryogenic distillation and the

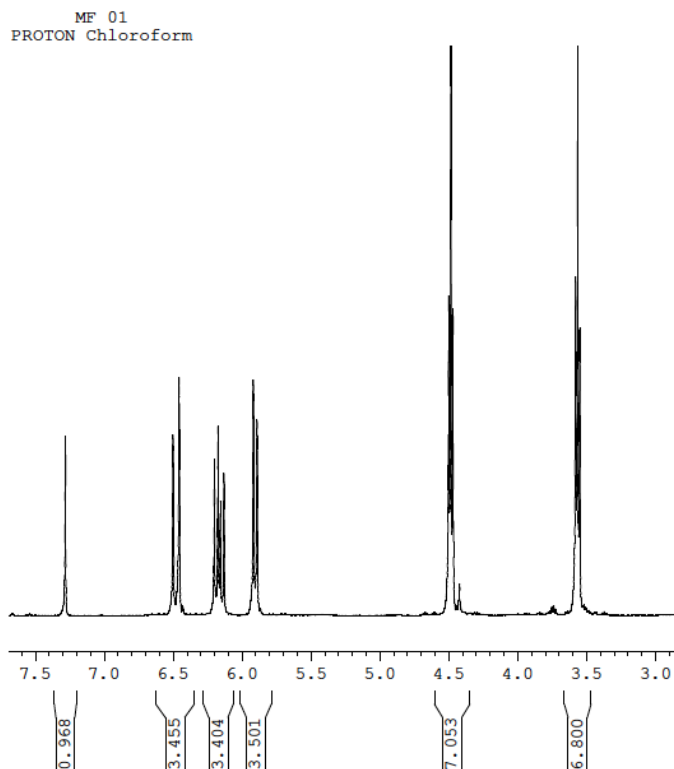
remaining 5 mL were poured into diethyl ether (150 mL) under vigorous stirring. The resulting purple precipitate was filtered and washed 5 times with diethyl ether, then dried under vacuum to give the compound VBRB as a purple solid.

**Synthesis of ethyl acrylate Rose Bengal (EARB) <sup>2</sup>**



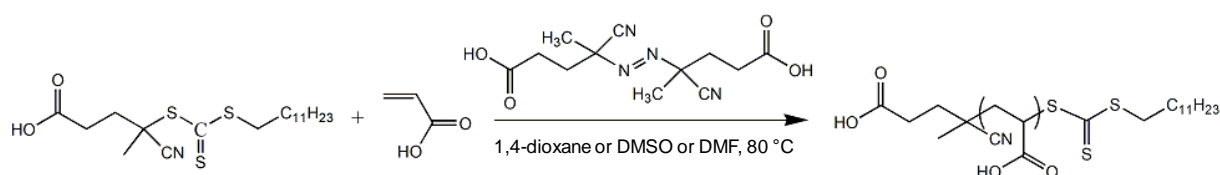
Scheme S 2. Synthesis of ethyl acrylate rose Bengal (EARB) monomer.

**Synthesis of 2-bromoethyl acrylate:** In a flamed 25 mL round bottom flask dried with a heat gun under a flow of argon, to a solution of 2-bromoethanol (0.858 mL, 12.1 mmol) in DCM (7 mL), TEA (1.858 mL, 13.3 mmol) was added and the reaction was cooled to 0 °C. Acryloyl chloride (1 mL, 11.9 mmol) in DCM (1 mL) was added dropwise over 1 h. The reaction was stirred overnight at room temperature, then filtered. The solid residue was washed with brine (2 x 10 mL) and the organic layer was dried over MgSO<sub>4</sub>. The solvent was removed under vacuum to give the 2-bromoethyl acrylate as a yellow liquid.



$^1\text{H}$  NMR spectrum of 2-bromoacrylate in  $\text{CDCl}_3$ .

**Synthesis of EARB:** In a 25 mL round bottom flask dried with a heat gun under a flow of argon, to a solution of RB (0.2 g, 0.2 mmol) in DMF (10 mL), 2-bromoethyl acrylate (0.107 g, 0.6 mmol) was added. The reaction mixture was degassed with a gentle flow of argon for 30 min, then stirred at 40 °C for 14 h. After cooling down to room temperature, 5 mL of the solvent were removed by cryogenic distillation, and the remaining 5 mL were poured into diethyl ether (250 mL) under vigorous stirring. Then, the mixture was stored in the fridge for 48 h. The resulting purple precipitate was filtered and washed 3 times with diethyl ether. It was dried under vacuum to give the EARB as a purple solid.



Scheme S 3. Synthesis of PAA-TTC polymers by RAFT polymerization mediated by 4-cyano-4-[(dodecylsulfanylthiocarbonyl)sulfanyl]pentanoic acid (trithiocarbonate chain transfer agent, TTC) and initiated by 4'-azobis(4-cyanopentanoic acid) (ACPA) initiator.

Table S 1. Experimental conditions and results for the RAFT polymerizations of acrylic acid, carried out at 80 °C.  $[AA]_0 = 2.8 \text{ mol.L}^{-1}$ .

Expt	Solvent	$[ACPA]_0$ ( $10^{-3} \text{ mol.L}^{-1}$ )	$[TTC]_0$ ( $10^{-2} \text{ mol.L}^{-1}$ )	$\frac{[TTC]_0}{[ACPA]_0}$	$\frac{[AA]_0}{[TTC]_0}$	Conv <sup>a</sup> (%)	$M_{n,th}$ <sup>b</sup> ( $\text{g.mol}^{-1}$ )	$M_{n,exp}$ <sup>c</sup> ( $\text{g.mol}^{-1}$ )	$\frac{M_{n,th}}{M_{n,exp}}$	$\bar{D}$
PAA-1	1,4-dioxane	7.1	7.2	10.1	40	68	2360	2320 <sup>d</sup>	1.0	1.2
PAA-2	1,4-dioxane	5.3	5.2	9.8	54	43	2080	2190 <sup>d</sup>	0.9	1.3
PAA-3	1,4-dioxane	4.0	3.9	9.6	72	93	5230	4960 <sup>d</sup>	1.1	1.3
PAA-4	1,4-dioxane	4.0	3.9	9.6	72	76	4360	5320 <sup>e</sup>	0.8	1.2
PAA-5	1,4-dioxane	4.1	3.9	9.6	72	56	3320	2690 <sup>e</sup>	1.2	1.2
PAA-6	1,4-dioxane	4.1	3.9	9.4	73	87	4960	3830 <sup>d</sup>	1.3	1.4
PAA-7	1,4-dioxane	2.4	2.3	9.3	124	60	5760	5330 <sup>e</sup>	1.1	1.5
PAA-8	DMSO	4.1	3.9	9.5	72	83	4680	3440 <sup>e</sup>	1.4	1.7
PAA-9	DMSO	3.9	3.9	9.9	72	90	5050	4070 <sup>e</sup>	1.2	1.3
PAA-10	DMF	4.0	3.9	9.7	72	88	4970	3440 <sup>d</sup>	1.4	1.4

<sup>a</sup> Conversion determined by <sup>1</sup>H NMR in DMSO-d<sub>6</sub> (Eq. 1 of main article). <sup>b</sup> Theoretical  $M_n$  of PAA-TTC calculated from Eq S. 20. <sup>c</sup>  $M_n$  of PAA-TTC recalculated from  $M_n$  of PMA-TTC (Eq S. 12) determined by SEC/polystyrene calibration in THF. <sup>d</sup> analysed with set No. 1 of columns, <sup>e</sup> analysed with set No. 2 of columns (see experimental part of the main article)

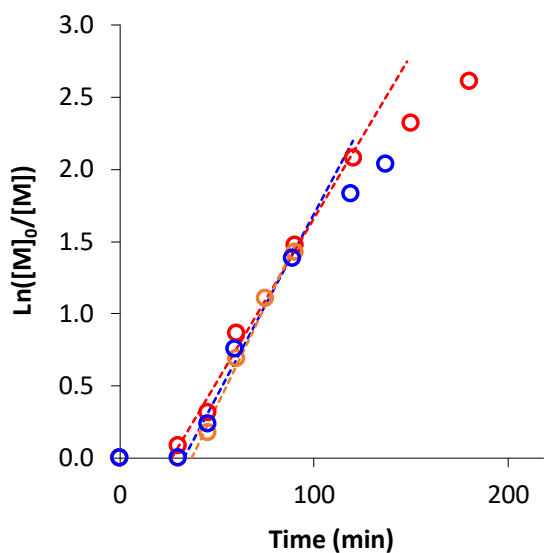


Figure S 1. Semilogarithmic conversion of monomer versus time for RAFT polymerizations of AA in 1,4-dioxane with ACPA concentration of: left)  $\text{red } \circ$   $4.0 \times 10^{-3} \text{ mol.L}^{-1}$  (PAA-3),  $\text{orange } \circ$   $4.0 \times 10^{-3} \text{ mol.L}^{-1}$  (PAA-4),  $\text{blue } \circ$   $4.1 \times 10^{-3} \text{ mol.L}^{-1}$  (PAA-6) (see Table S 1).

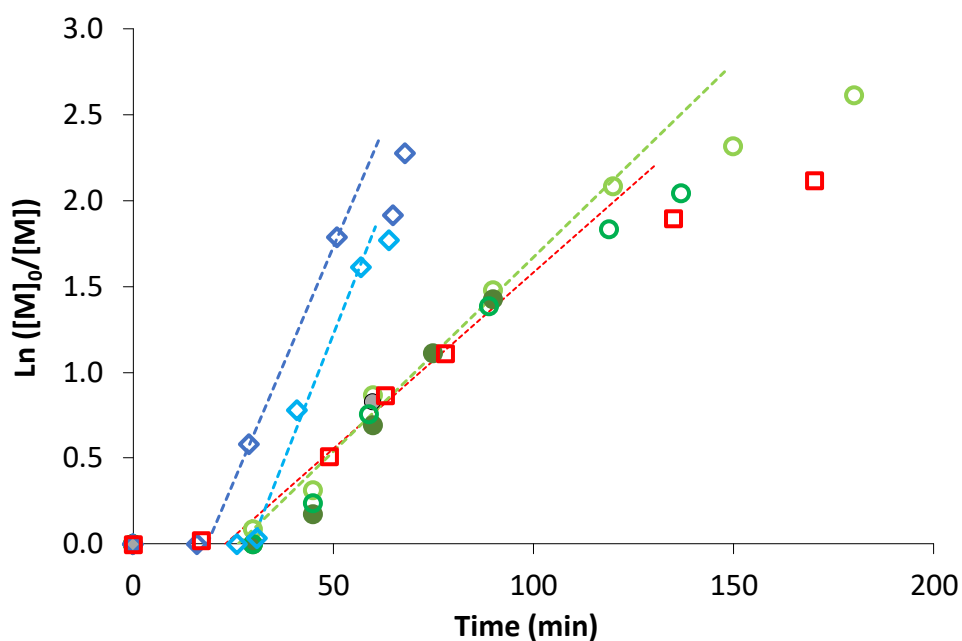


Figure S 2. Semilogarithmic conversion of monomer versus time for RAFT polymerizations of AA in 1,4-dioxane ( $\text{green } \circ$  PAA-3,  $\text{dark green } \bullet$  PAA-4,  $\text{black } \bullet$  PAA-5,  $\text{light green } \circ$  PAA-6), DMSO ( $\text{light blue } \diamond$  PAA-8,  $\text{dark blue } \diamond$  PAA-9) or DMF ( $\text{red } \square$  PAA-10) (see Table S 1).

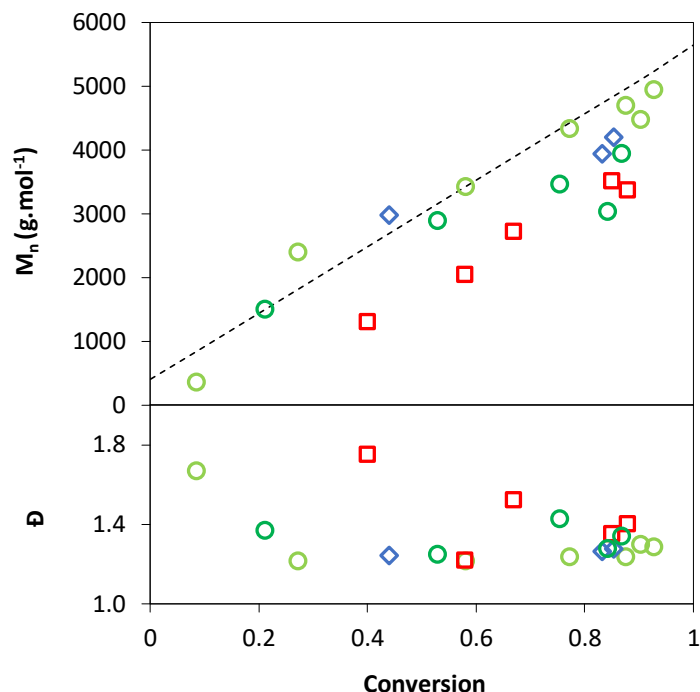


Figure S 3. Evolution of the number-average molar mass and the dispersity versus monomer conversion for RAFT polymerization of AA in 1,4-dioxane (○ PAA-3, ○ PAA-6), DMSO (◇ PAA-9) or DMF (□ PAA-10). Dotted line corresponds to theoretical number-average molar masses (Eq S. 20).  $M_n$  derived from analysis of methylated PAA using PS calibration (Eq S. 12).

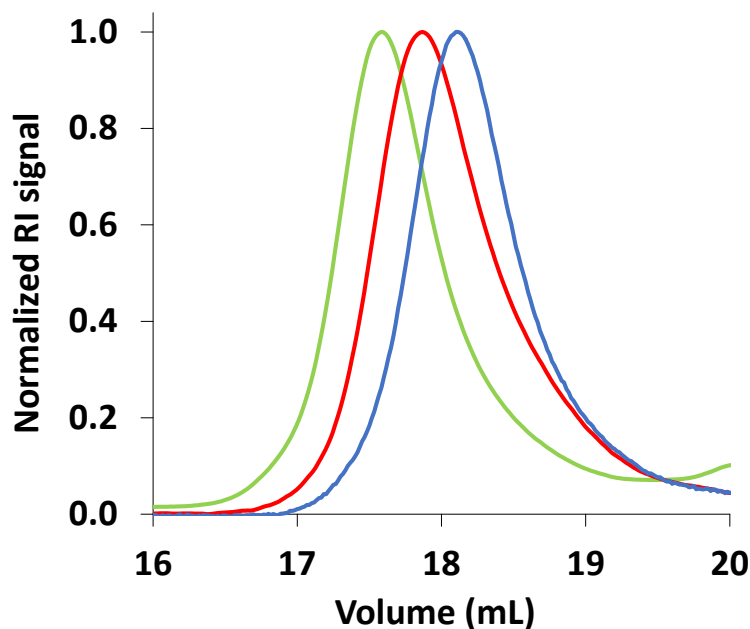


Figure S 4. Overlay of SEC chromatograms of purified methylated PAA-TTC synthesized in 1,4-dioxane (— green line,  $x = 93\%$ , PAA-3), DMF (— red line,  $x = 88\%$ , PAA-10) or DMSO (— blue line,  $x = 90\%$ , PAA-5). SEC analyses carried out in THF eluent at  $30\text{ }^\circ\text{C}$  with set No.1 of SEC columns.

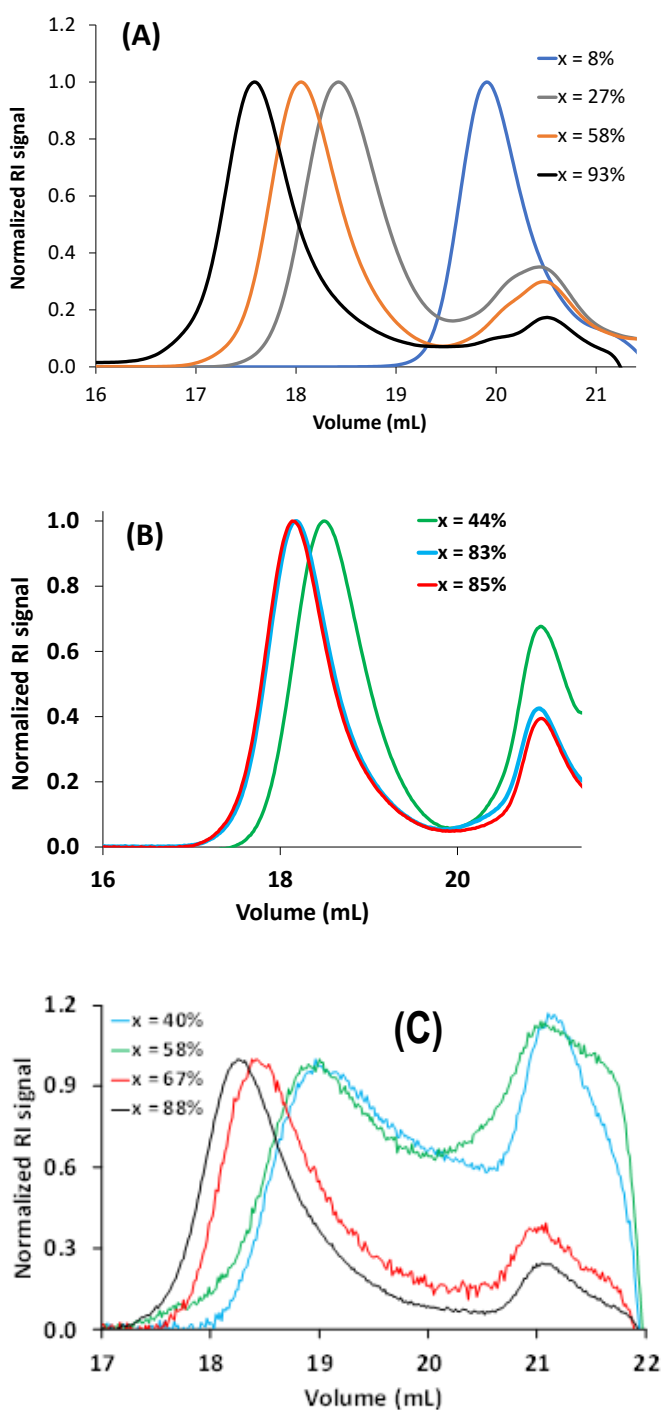


Figure S 5. Evolution of normalized SEC chromatograms with monomer conversion ( $x$ ) for RAFT polymerization of AA in (A) 1,4-dioxane (PAA-3), (B) DMSO (PAA-9) and (C) DMF (PAA-10) (Table S 1). SEC analyses carried out in THF at 30 °C using a refractive index detector and polystyrene calibration. Set 1 of SEC columns.

Note that the extra peak observed in all SEC chromatograms between 20 and 21 mL was ascribed to residual trimethyl(silyl) diazomethane used to methylate the carboxylic acid functions of PAA-TTC. This peak was indeed observed also for SEC chromatograms of precipitated methylated PAA and PAA-*b*-PnBA with a characteristic UV-visible trace at 310 nm.

Table S 2. Normalized polarity values and polarizability parameters of solvents.

Solvent	$E_T^N$ <sup>a</sup>	$\pi^*$ <sup>b</sup>
1,4-dioxane	0.164	0.55
DMF	0.386	0.88
DMSO	0.444	1.00

<sup>a</sup> Normalized polarity value, calculated using water and tetramethylsilane (TMS) as extreme polar and nonpolar reference solvents (reference <sup>4</sup>), <sup>b</sup> Polarizability parameter (reference <sup>5</sup>).



Table S 3. Experimental conditions and results for the RAFT copolymerizations of AA with RB-based co-monomer (MRB) in 1,4-dioxane, DMSO or DMF at 80 °C.  $[AA]_0 = 2.8$  to  $2.9 \text{ mol.L}^{-1}$ .

Expt	Solvent	MRB	$f_{MRB,0}^b$ (mol-%)	$[ACPA]_0$ ( $10^{-3} \text{ mol.L}^{-1}$ )	$[TTC]_0$ ( $10^{-2} \text{ mol.L}^{-1}$ )	$\frac{[MRB]_0}{[ACPA]_0}$	$\frac{[TTC]_0}{[ACPA]_0}$	$\frac{[AA]_0}{[TTC]_0}$	Conv <sup>c</sup> (%)	$M_{n,th}^d$ ( $\text{g.mol}^{-1}$ )	$M_{n,PS}^{e,g}$ ( $\text{g.mol}^{-1}$ )	$\bar{D}^f$
PAA-RB	1,4-dioxane	Non-polymerizable RB	0.47	4.0	4.0	3.4	10.1	70	81	4520	ND	ND
PAA-EARB5 <sup>a</sup>	1,4-dioxane	EARB	0.05	4.0	4.0	0.4	10.1	70	90	4940	3990	1.5
PAA-EARB6	1,4-dioxane	EARB	0.21	2.5	2.3	2.4	9.3	121	34	3320	ND	ND
PAA-EARB7	1,4-dioxane	EARB	0.40	4.3	2.3	2.8	9.4	70	49	2840	ND	ND
PAA-VBRB3	1,4-dioxane	VBRB	0.50	4.2	4.0	3.3	9.4	73	8	ND	ND	ND
PAA-VBRB4 <sup>a</sup>	1,4-dioxane	VBRB	0.50	4.3	4.0	3.3	9.4	70	7	ND	ND	ND
PAA-EARB8	DMSO	EARB	0.25	4.2	4.0	1.7	9.6	70	85	4690	ND	ND
PAA-VBRB5	DMSO	VBRB	0.10	4.1	3.9	0.7	9.6	71	70	3990	3670	1.3
PAA-VBRB6 <sup>a</sup>	DMSO	VBRB	0.25	4.3	4.0	1.6	9.4	70	90	4940	4080	1.4

PAA- EARB9	DMF	EARB	0.25	6.7	6.8	1.0	10.0	40	56	2330	ND	ND
PAA- VBRB7	DMF	VBRB	0.25	4.0	4.0	1.8	10.1	70	62	3530	ND	ND

<sup>a</sup> Synthesis carried out in dark. <sup>b</sup> Initial molar fraction of MRB versus AA,  $f_{\text{MRB},0} = n_{\text{MRB},0} / (n_{\text{MRB},0} + n_{\text{AA},0})$ . <sup>c</sup> Conversion determined by <sup>1</sup>H NMR in DMSO-d<sub>6</sub> (Eq. 1 of article). <sup>d</sup> Theoretical  $M_n$  of P(AA-co-MRB)-TTC calculated from Eq S. 20. <sup>e</sup>  $M_n$  of P(AA-co-MRB)-TTC recalculated from  $M_n$  of P(MA-co-MRB)-TTC determined by SEC/polystyrene calibration in THF (Eq S. 12). <sup>f</sup> Dispersity ( $\mathcal{D} = M_w/M_n$ ). <sup>g</sup> Analysed with set No. 1 of columns (see experimental part of article)

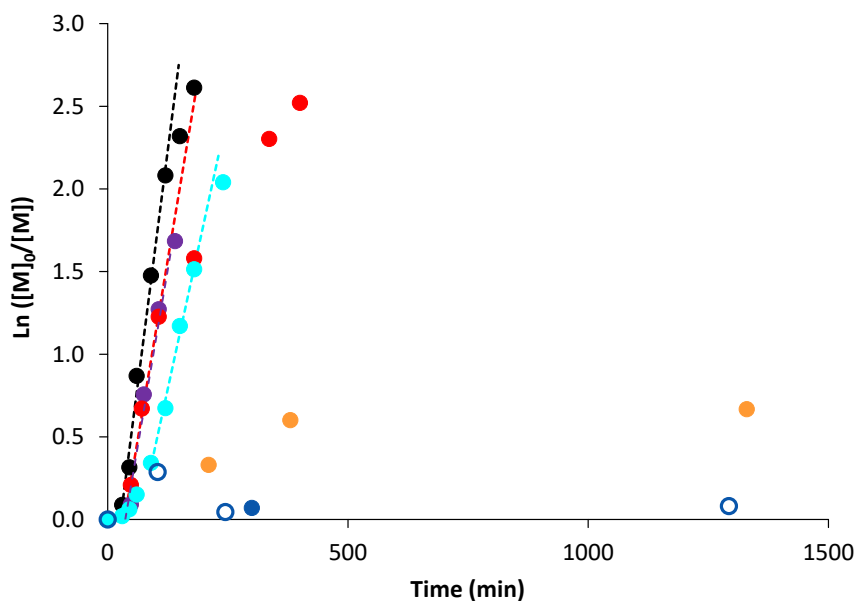


Figure S 6. Semilogarithmic conversion of acrylic acid versus time for the RAFT (co)polymerization in 1,4-dioxane of AA with: 0 mol% of MRB (● PAA-3), 0.47 mol% of free RB (● PAA-RB), 0.10 mol% of EARB (● PAA-EARB1), 0.40 mol% of EARB (● PAA-EARB7), 0.10 mol% of VBRB (● PAA-VBRB1), 0.50 mol% of VBRB (● PAA-VBRB3) and 0.50 mol% of VBRB (○ PAA-VBRB4, polymerization carried out in dark) (see Table 1, Table S 1 and Table S 3).

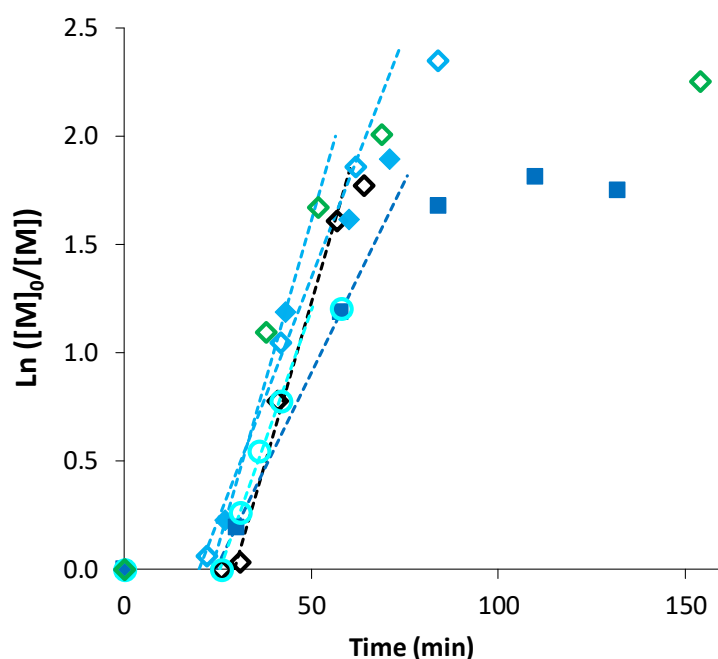


Figure S 7. Semilogarithmic conversion of acrylic acid versus time for the RAFT (co)polymerization in DMSO of AA with increasing fraction of MRB. Plain symbols for EARB (0.25 mol-% (◆ PAA-EARB8), 0.36 mol-% (■ PAA-EARB4)) and empty symbols for VBRB (0.10 mol-% (○ PAA-VBRB5), 0.25 mol-% (◇ PAA-VBRB6 and ◇ PAA-VBRB2)). The black empty diamonds correspond to 0 mol-% of MRB (◇ PAA-8).

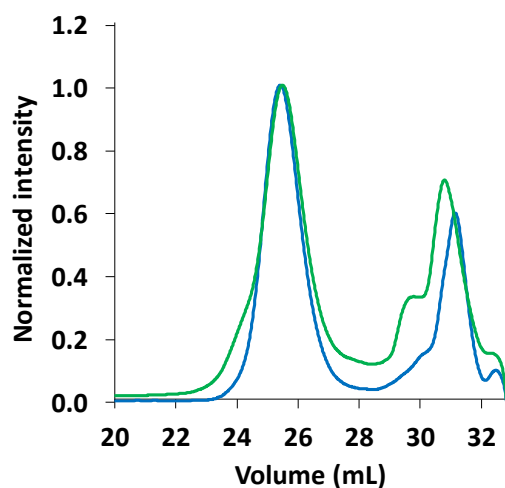


Figure S 8. Overlay of RI traces of SEC chromatograms of methylated precipitated P(AA-co-VBRB<sub>0.25%</sub>)-TTC (— PAA-VBRB2) and P(AA-co-EARB<sub>0.36%</sub>)-TTC (— PAA-EARB4). Analysed with set No.2 of SEC columns. The signal between 29 – 32 mL is ascribed to residual trimethyl(silyl) diazomethane.

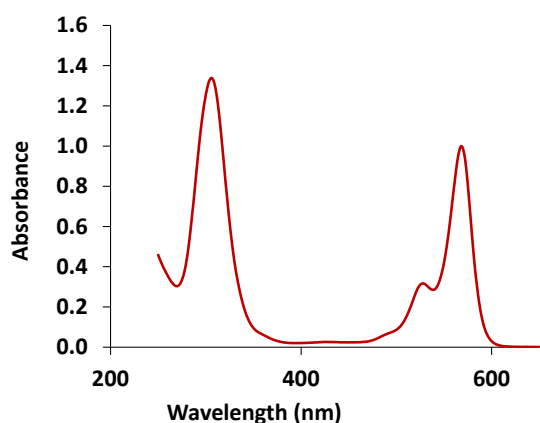
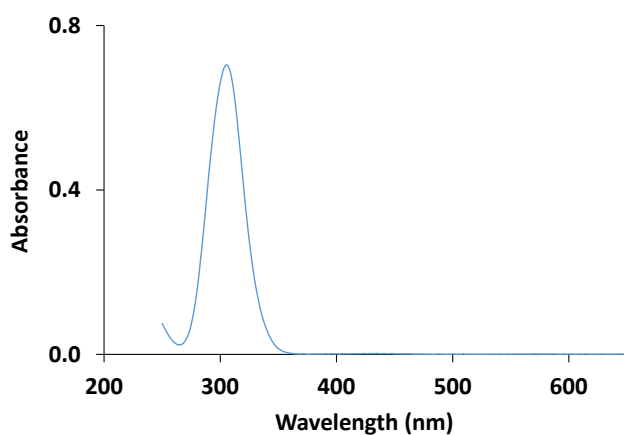


Figure S 9. Examples of absorbance spectra of (top) PAA-TTC and (bottom) P(AA-co-EARB 0.25%) (PAA-EARB9) in ethanol.

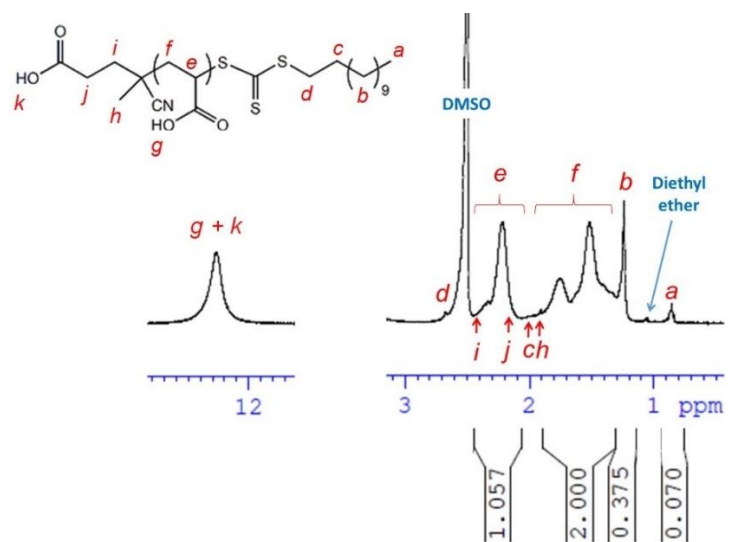


Figure S 10.  $^1\text{H}$  NMR spectrum in  $\text{DMSO-d}_6$  of PAA-TTC synthesized by RAFT polymerization in 1,4-dioxane and purified by precipitation in diethyl ether (PAA-4 in Table S 1).

Table S 4. Average number of trithiocarbonate (TTC) functions per PAA-based polymer chain.

Expt	Polymer	Solvent of RAFT polymerization	$N_{TTC/chain}$		
			UV <sub>EtOH</sub> b	<sup>1</sup> H NMR c	PE (%) e
PAA-1	PAA-TTC	1,4-dioxane	1.1	1.2	8
PAA-2	PAA-TTC	1,4-dioxane	1.0	1.0	0
PAA-3	PAA-TTC	1,4-dioxane	1.0	1.8	44
PAA-4	PAA-TTC	1,4-dioxane	0.6	1.6	62
PAA-5	PAA-TTC	1,4-dioxane	1.1	1.3	15
PAA-6	PAA-TTC	1,4-dioxane	0.6	0.8	25
PAA-7	PAA-TTC	1,4-dioxane	0.9	0.7	28
PAA-EARB5 <sup>a</sup>	P(AA-co-EARB <sub>0.05%</sub> )-TTC	1,4-dioxane	0.9	0.9	0
PAA-EARB1	P(AA-co-EARB <sub>0.1%</sub> )-TTC	1,4-dioxane	0.9	1.5	40
PAA-EARB2	P(AA-co-EARB <sub>0.1%</sub> )-TTC	1,4-dioxane	0.9	1.2	25
PAA-EARB3	P(AA-co-EARB <sub>0.1%</sub> )-TTC	1,4-dioxane	0.8	1.1	27
PAA-VBRB1	P(AA-co-VBRB <sub>0.1%</sub> )-TTC	1,4-dioxane	0.8	1.0	20
PAA-8	PAA-TTC	DMSO	1.3	0.9	44
PAA-9	PAA-TTC	DMSO	1.2	0.9	33
PAA-EARB8	P(AA-co-EARB <sub>0.25%</sub> )-TTC	DMSO	1.5 <sup>d</sup>	1.3 <sup>d</sup>	15
PAA-EARB4 <sup>a</sup>	P(AA-co-EARB <sub>0.36%</sub> )-TTC	DMSO	1.4	1.2	16
PAA-VBRB5	P(AA-co-VBRB <sub>0.1%</sub> )-TTC	DMSO	1.0	0.9	11
PAA-VBRB6 <sup>a</sup>	P(AA-co-VBRB <sub>0.25%</sub> )-TTC	DMSO	1.2	0.8	50
PAA-VBRB2 <sup>a</sup>	P(AA-co-VBRB <sub>0.25%</sub> )-TTC	DMSO	1.6	1.3	23

PAA-10	PAA-TTC	DMF	0.8	0.8	0
PAA-EARB9	P(AA-co-EARB <sub>0.25%</sub> )-TTC	DMF	1.4 <sup>d</sup>	1.1 <sup>d</sup>	27
PAA-VBRB7	P(AA-co-VBRB <sub>0.25%</sub> )-TTC	DMF	1.1 <sup>d</sup>	1.0 <sup>d</sup>	10

<sup>a</sup> Synthesis carried out in dark. <sup>b</sup> Average number of TTC functions per PAA-based chain determined by UV-visible spectroscopy in ethanol from **Erreur ! Source du renvoi introuvable.** and Figure S 9, <sup>c</sup> Average number of TTC functions per PAA-based chain determined by proton NMR in deuterated methanol (MeOD) from Figure S 10. <sup>d</sup> Values determined from theoretical  $M_{n,theo}$  as experimental  $M_n$  was not determined by SEC for those samples. The error is minimized as results of Table S1 and Table S3 shows theoretical  $M_n$  close to experimental  $M_n$  is close to 1. <sup>e</sup> Percent relative error between  $N_{TTC/chain}$  measured by either UV-visible absorbance or by 1H NMR.

*Determination of number of TTC group per chain by UV-visible spectroscopy (see Figure S 9):*

$$N_{TTC/chain} (UV) = \frac{C_{mol,TTC} \times M_{n,SEC}}{C_{wt,polymer}} \quad \text{Eq S. 1}$$

$C_{mol,TTC}$  is the molar concentration of TTC group calculated from Beer-Lambert law at 307 nm assuming that the molar absorption coefficient of the TTC chain end is similar to the one of the molecular trithiocarbonate chain transfer agent measured in ethanol ( $\epsilon_{TTC, EtOH} = 11\,306 \text{ L}\cdot\text{mol}^{-1}\cdot\text{cm}^{-1}$ ),  $C_{wt,Polymer}$  is the weight concentration of PAA-based polymer in the UV cuvette, and  $M_{n,SEC}$  is the number-average molar mass of the polymer (PAA or P(AA-co-MRB)) determined by SEC analysis of the methylated polymer based on a polystyrene calibration (see experimental part and Table S 1 and Table S 4).

*Determination of number of TTC group per chain by 1H NMR (see Figure S 10):*

The ratio between the peak area of the chain end and the number of moles of PAA chains allowed us to determine the chain end functionalization of PAA (**Erreur ! Source du renvoi introuvable.**).

$$N_{TTC/chain} (NMR) = \frac{I_a/3}{(I_e+I_f)/3} \times DP_{n,SEC} \quad \text{Eq S. 2}$$

The term  $I_a$  corresponds to the integration of the methyl group of the chain end alkyl group (protons  $a$ ) of the TTC,  $I_e$  and  $I_f$  are the integration of the protons of the PAA backbone (Figure S 10).  $DP_{n,SEC}$  is the number-average degree of polymerization calculated from  $M_{n,SEC}$  and molar mass of monomer units.



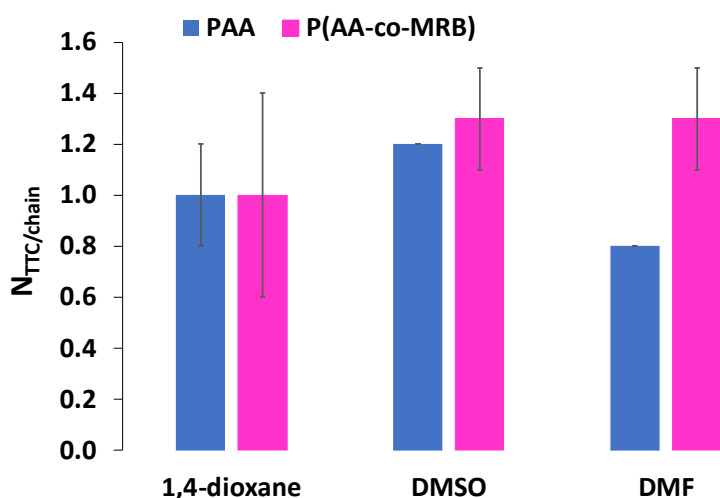


Figure S 11. Comparison of the average number of TTC per polymer chain determined by UV-visible spectroscopy in ethanol for PAA and RB-based PAA synthesized in 1,4-dioxane, DMSO or DMF. Error bars represent standard deviation based on data of Table S 4.

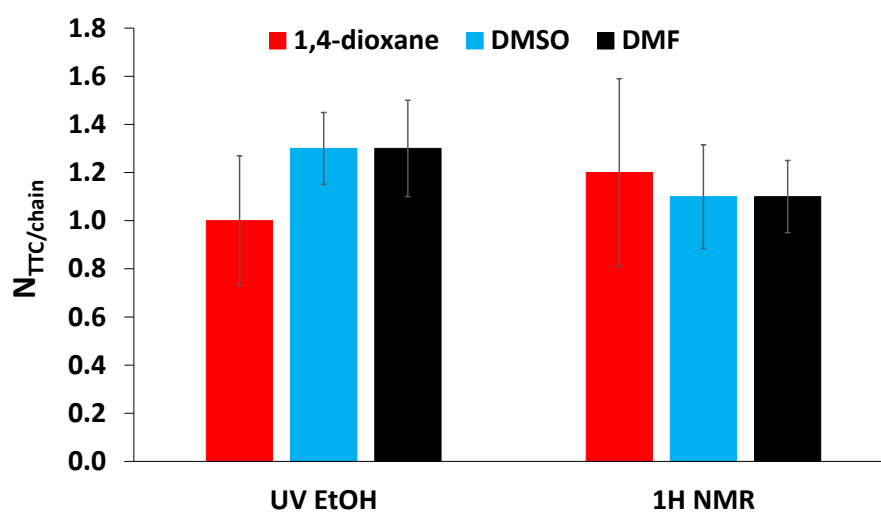


Figure S 12. Comparison of the average number of TTC functions per P(AA-co-MRB) chain determined by either UV-visible spectroscopy in ethanol (Equation (1)) or by  $^1H$  NMR in DMSO- $d_6$  (Equation (2)), according to the solvent of copolymer synthesis (1,4-dioxane, DMSO, DMF) (see Figure S 9 and Figure S 10) . The error bar represents the standard deviation based on data of Table S 4.

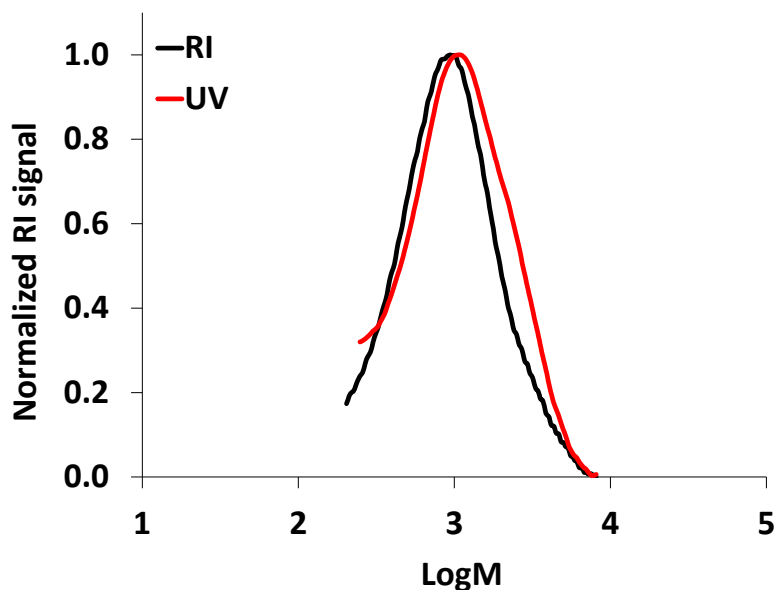


Figure S 13. Molar mass distribution of P(AA-*co*-EARB<sub>0.21%</sub>)-TTC synthesized by RAFT polymerization in 1,4-dioxane (PAA-EARB6, Table S3). SEC performed with set No. 1 of columns. The black line corresponds to the refractometer trace and the red trace corresponds to the absorbance at 570 nm (UV-visible detector) characteristic of RB moiety.

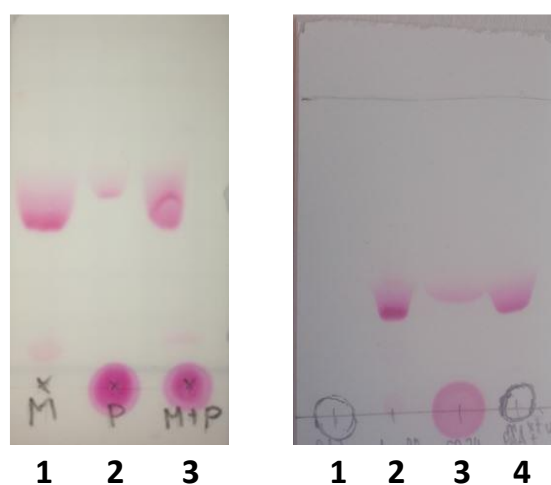


Figure S 14. Thin layer chromatography with methanol/acetone/chloroform (10/10/80 v/v/v) as mobile phase. Left) (1) EARB solution in acetone, (2) crude P(AA-*co*-EARB<sub>0.4%</sub>)-TTC copolymer (PAA-EARB7 in Table S 3) in 1,4-dioxane, (3) mixture of (1) and (2). Right) (1) crude PAA-TTC (PAA-5, Table S1 and table S2) in 1,4-dioxane, (2) EARB in 1,4-dioxane, (3) purified P(AA-*co*-EARB<sub>0.21%</sub>)-TTC copolymer (PAA-EARB6 in Table S 3) in water, (4) mixture of (1) and (2).

Table S 5. Characterization of the composition in photosensitizer of P(AA-co-MRB)-TTC statistical copolymers synthesized by RAFT polymerization at 80 °C.

Expt	Solvent	Polymer	Theor. RB loading <sup>b</sup> ( $\mu\text{mol}\cdot\text{g}^{-1}$ )	Exp. RB loading <sup>c</sup> ( $\mu\text{mol}\cdot\text{g}^{-1}$ )	$F_{MRB}$ <sup>d</sup> (mol-%)	$N_{MRB/chain}$ <sup>e</sup>
PAA-EARB5 <sup>a</sup>	1,4-dioxane	P(AA-co-EARB <sub>0.05%</sub> )-TTC	6	5	0.03	0.02
PAA-EARB1	1,4-dioxane	P(AA-co-EARB <sub>0.1%</sub> )-TTC	13	7	0.05	0.03
PAA-EARB2	1,4-dioxane	P(AA-co-EARB <sub>0.1%</sub> )-TTC	13	6	0.04	0.03
PAA-EARB3	1,4-dioxane	P(AA-co-EARB <sub>0.1%</sub> )-TTC	14	8	0.06	0.05
PAA-VBRB1	1,4-dioxane	P(AA-co-VBRB <sub>0.1%</sub> )-TTC	13	6	0.04	0.02
PAA-EARB8	DMSO	P(AA-co-EARB <sub>0.25%</sub> )-TTC	30	22	0.16	0.10 <sup>f</sup>
PAA-EARB4 <sup>a</sup>	DMSO	P(AA-co-EARB <sub>0.36%</sub> )-TTC	45	33	0.23	0.14
PAA-VBRB5	DMSO	P(AA-co-VBRB <sub>0.1%</sub> )-TTC	13	10	0.07	0.04
PAA-VBRB6 <sup>a</sup>	DMSO	P(AA-co-VBRB <sub>0.25%</sub> )-TTC	31	27	0.19	0.11
PAA-VBRB2 <sup>a</sup>	DMSO	P(AA-co-VBRB <sub>0.25%</sub> )-TTC	31	31	0.22	0.16
PAA-EARB9	DMF	P(AA-co-EARB <sub>0.25%</sub> )-TTC	37	31	0.22	0.07 <sup>f</sup>
PAA-VBRB7	DMF	P(AA-co-VBRB <sub>0.25%</sub> )-TTC	33	23	0.16	0.08 <sup>f</sup>

<sup>a</sup> Experiments carried out in dark. <sup>b</sup> Theoretical RB loading of macroCTA (Eq S. 5). <sup>c</sup> Experimental weight RB loading per mass of macroCTA determined from UV-visible spectroscopy carried out in ethanol (Erreur ! Source du renvoi introuvable.). <sup>d</sup> Final molar fraction of MRB in P(AA-co-MRB) determined by UV-UV-visible spectroscopy carried out in ethanol (Eq S. 6). <sup>e</sup> Average number of MRB units per polymer chain determined by UV-UV-visible spectroscopy carried out in ethanol (Eq S. 7). <sup>f</sup> Values determined from theoretical  $M_n$ .

The MRB loading ( $\mu\text{mol MRB}\cdot\text{g}_{\text{polymer}}^{-1}$ ) was determined from UV-vis spectra following **Erreur ! Source du renvoi introuvable.**

$$\text{Exp. MRB loading } (\mu\text{mol}\cdot\text{g}_{\text{polymer}}^{-1}) = \frac{C_{\text{mol,MRB}}}{C_{\text{wt,polymer}}} = \frac{\text{Abs}/(\varepsilon_{\text{RB},549\text{nm}}\times l)}{m/V} \quad \text{Eq S. 3}$$

with  $C_{\text{mol,MRB}}$  the molar concentration of MRB calculated from Beer-Lambert law in 1 cm UV cuvette assuming that the molar extinction coefficient of MRB was the same as that of RB ( $\varepsilon_{\text{RB } 549 \text{ nm,water}} = 113\,598 \text{ L}\cdot\text{mol}^{-1}\cdot\text{cm}^{-1}$ ),  $C_{\text{wt,polymer}}$  the weight concentration of polymer (PAA and PAA-TTC) in the UV cuvette. The concentration  $C_{\text{MRB}}$  of MRB was determined from the absorbance at 559 nm through the Beer-Lambert equation (Eq S. 4),

$$A_{559 \text{ nm}} = \varepsilon_{\text{RB}} C_{\text{MRB}} l \quad \text{Eq S. 4}$$

with  $A_{559 \text{ nm}}$  the absorbance,  $\varepsilon_{\text{RB}}$  the molar extinction coefficient of RB in water and  $l$  the path length ( $l = 1 \text{ cm}$ ).

The theoretical RB loading was calculated from Eq S. 5.

$$\text{Theor. MRB loading } (\text{mol}\cdot\text{g}_{\text{polymer}}^{-1}) = \frac{n_{\text{MRB},0}}{m_{\text{monomers},0} + m_{\text{RAFT agent},0}} \quad \text{Eq S. 5}$$

with  $n_{\text{MRB},0}$  the initial number of moles of MRB,  $m_{\text{monomers},0}$  and  $m_{\text{RAFT agent},0}$  the initial masses of monomers and RAFT agent introduced in the initial mixture.

The composition of the copolymer, *i.e.* the average molar fraction of MRB per PAA unit ( $F_{\text{MRB}}$ ) was determined by UV-vis analyses in cuvette in water or in ethanol following

Eq S. 6.

$$F_{\text{MRB}} (\text{UV})(\text{mol}\%) = \frac{C_{\text{mol,MRB}}}{C_{\text{wt,polymer}}/M_{\text{AA}} + C_{\text{mol,MRB}}} \quad \text{Eq S. 6}$$

$M_{\text{AA}}$  is the molar mass of AA ( $M_{\text{AA}} = 72 \text{ g}\cdot\text{mol}^{-1}$ ).

The number of MRB units per polymer chain was calculated from Eq S. 7:

$$N_{MRB/chain} (UV) = \frac{C_{mol,MRB} \times M_{n,SEC}}{C_{wt,polymer}} = Exp. MRB loading \times M_{n,SEC} \quad Eq S. 7$$

$M_{n,SEC}$  is the number-average molar mass of the polymer determined by SEC/PS calibration in THF ( Eq S. 7).

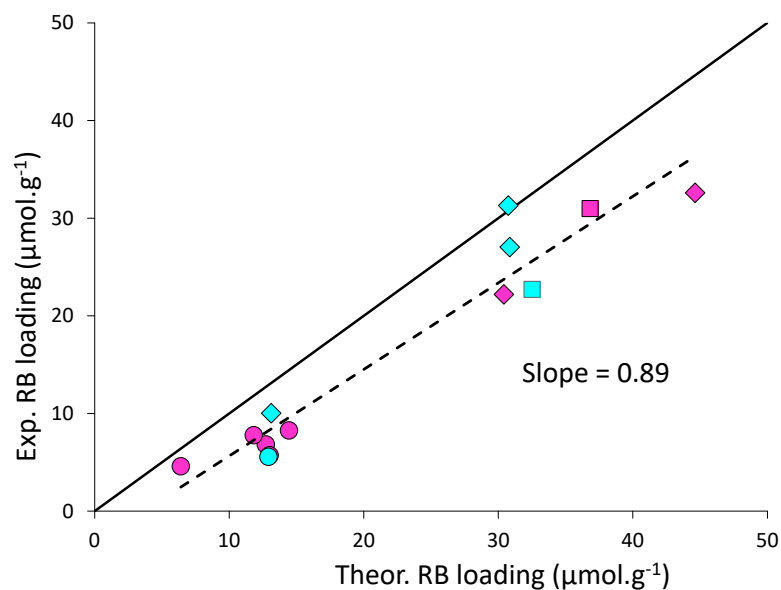


Figure S 15. Experimental RB loading determined by UV-vis in cuvette in ethanol versus theoretical RB loading for P(AA-co-EARB)-TTC synthesized in 1,4-dioxane (●), DMSO (◆) or DMF (■); P(AA-co-VBRB)-TTC synthesized in 1,4-dioxane (●), DMSO (◆) or DMF (■). The full line represents the bisector, the dotted line represents the linear regression.

Table S 6. Experimental conditions for the emulsion polymerization of *n*BA and/or EA mediated by PAA-TTC, carried out at 70 °C with 23 wt-% of targeted solids content at 100% monomer conversion. Initial pH = 5.4 (adjusted with NH<sub>4</sub>OH).

INITIAL MACRO-CTA				FINAL WATERBORNE LATEX							
PAA-TTC	Solvent of AA RAFT	$M_{n,PAA-TTC}$ <sup>a</sup> (g.mol <sup>-1</sup> )	Đ	Latex	Polymer	$\omega_{PAA-TTC}$ <sup>b</sup> (wt-%)	[ACPA] <sub>0</sub> (10 <sup>-4</sup> mol.L <sub>H2O</sub> <sup>-1</sup> )	[Monomer] (mol.L <sub>H2O</sub> <sup>-1</sup> )	[PAA-TTC] <sub>0</sub> (10 <sup>-3</sup> mol.L <sub>H2O</sub> <sup>-1</sup> )	$\frac{[PAA-TTC]}{[ACPA]_0}$	$\frac{n_{monomer,0}}{n_{PAA-TTC,0}}$
PAA-5	1,4-dioxane	2690	1.2	LBA-8	PAA- <i>b</i> -PnBA	2.8	6.1	2.4	4.3	7.1	551
PAA-4	1,4-dioxane	5320	1.2	LBA-9 <sup>c</sup>	PAA- <i>b</i> -PnBA	5.3	7.2	2.5	3.4	4.7	749
PAA-4	1,4-dioxane	5320	1.2	LBA-10	PAA- <i>b</i> -PnBA	5.8	7.2	2.5	3.6	5.0	700
PAA-9	DMSO	4070	1.3	LBA-11	PAA- <i>b</i> -PnBA	2.4	6.1	2.4	1.7	2.8	1404
PAA-8	DMSO	3440	1.7	LBA-12	PAA- <i>b</i> -PnBA	4.4	7.1	2.5	4.3	6.1	587
PAA-8	DMSO	3440	1.7	LBAEA-13	PAA- <i>b</i> - P( <i>n</i> BA <sub>70%</sub> /EA <sub>30%</sub> )	4.8	7.9	2.7	4.6	5.9	587
PAA-5	1,4-dioxane	2690	1.2	LEA-14	PAA- <i>b</i> -PEA	2.2	3.2	3.1	2.3	7.2	1320
PAA-4	1,4-dioxane	5320	1.2	LEA-15	PAA- <i>b</i> -PEA	6.6	7.8	3.2	4.3	5.5	747
PAA-9	DMSO	4070	1.3	LEA-16	PAA- <i>b</i> -PEA	2.8	7.8	3.0	2.2	2.8	1413
PAA-10	DMF	3440	1.4	LEA-17	PAA- <i>b</i> -PEA	4.7	8.5	3.1	4.4	5.2	693

<sup>a</sup> Experimental  $M_n$  of PAA-TTC macroCTA determined by SEC/PS calibration in THF (see Chapter 2). <sup>b</sup> Final PAA-TTC weight fraction =  $m_0(\text{PAA-TTC}) / [m_0(\text{PAA-TTC}) + m_0(\textit{nBA or EA}) \times \text{conversion}]$ . <sup>c</sup> Synthesis performed under nitrogen flow.

Table S 7. Experimental results for the emulsion polymerization of either *n*BA or EA or *n*BA/EA stabilized with PAA-TTC, carried out at 70 °C with 23 wt-% of targeted solids content at 100% monomer conversion. Initial pH = 5.4 (adjusted with NH<sub>4</sub>OH).

Expt	Polymer	Conv <sup>a</sup> (%)	$M_{n,th}$ <sup>b</sup> (kg.mol <sup>-1</sup> )	$M_{n,PS}$ <sup>c</sup> (kg.mol <sup>-1</sup> )	$\mathfrak{D}_{PS}$ <sup>f</sup>	$M_{n,MALLS}$ <sup>g</sup> (kg.mol <sup>-1</sup> )	$\mathfrak{D}_{MALLS}$ <sup>h</sup>	$D_h$ <sup>i</sup> (nm) (PDI)	$N_p$ <sup>j</sup> (10 <sup>17</sup> L <sub>latex</sub> <sup>-1</sup> )
LBA-8	PAA- <i>b</i> -P <i>n</i> BA	100	73	147 <sup>d</sup>	6.1	570 <sup>d</sup>	2.2	98 (0.11)	4.4
LBA-9	PAA- <i>b</i> -P <i>n</i> BA	100	101	96 <sup>e</sup>	2.7	170 <sup>e</sup>	2.0	105 (0.06)	3.7
LBA-10	PAA- <i>b</i> -P <i>n</i> BA	96	91	125 <sup>d</sup>	2.8	251 <sup>d</sup>	1.7	74 (0.03)	10.1
LBA-11	PAA- <i>b</i> -P <i>n</i> BA	93	172	137 <sup>e</sup>	3.2	342 <sup>e</sup>	1.4	93 (0.06)	4.8
LBA-12	PAA- <i>b</i> -P <i>n</i> BA	100	79	114 <sup>e</sup>	4.1	194 <sup>e</sup>	1.7	90 (0.06)	5.9
LBAEA-13	PAA- <i>b</i> -P( <i>n</i> BA <sub>30%</sub> - <i>co</i> - EA <sub>70%</sub> )	97	71	148 <sup>e</sup>	4.3	249 <sup>e</sup>	1.8	91 (0.05)	5.4
LEA-15	PAA- <i>b</i> -PEA	100	80	80 <sup>e</sup>	2.9	128 <sup>e</sup>	1.6	92 (0.07)	5.0
LEA-16	PAA- <i>b</i> -PEA	100	145	95 <sup>e</sup>	4.9	132 <sup>e</sup>	2.3	95 (0.07)	4.4
LEA-17	PAA- <i>b</i> -PEA	100	73	82 <sup>e</sup>	4.1	129 <sup>e</sup>	2.0	96 (0.09)	4.3

<sup>a</sup> Monomer conversion calculated by gravimetry (Eqn 2 of article), <sup>b</sup> Theoretical  $M_n$  of block copolymers calculated from Eq S. 21 and Eq S. 22, <sup>c, g</sup> Experimental  $M_n$  of block copolymers recalculated from  $M_n$  of methylated block copolymers determined by SEC in THF (Eq S. 13), <sup>e</sup> Values obtained by SEC from a refractometer detector using PS calibration, <sup>g</sup> Values obtained by SEC from a MALLS detector,  $(dn/dc)_{copo}$  calculated from  $dn/dc$  values of PMA and P*n*BA (Eq S. 18). <sup>d</sup> analysed with set No.2 of columns, <sup>e</sup> analysed with set No. 1 of columns, see experimental part. <sup>f, h</sup> dispersity ( $\mathfrak{D} = M_w/M_n$ ). <sup>i</sup> Hydrodynamic diameter of particles measured by DLS. <sup>j</sup> Average number of particles determined from  $D_h$  (eqn 7 of article).

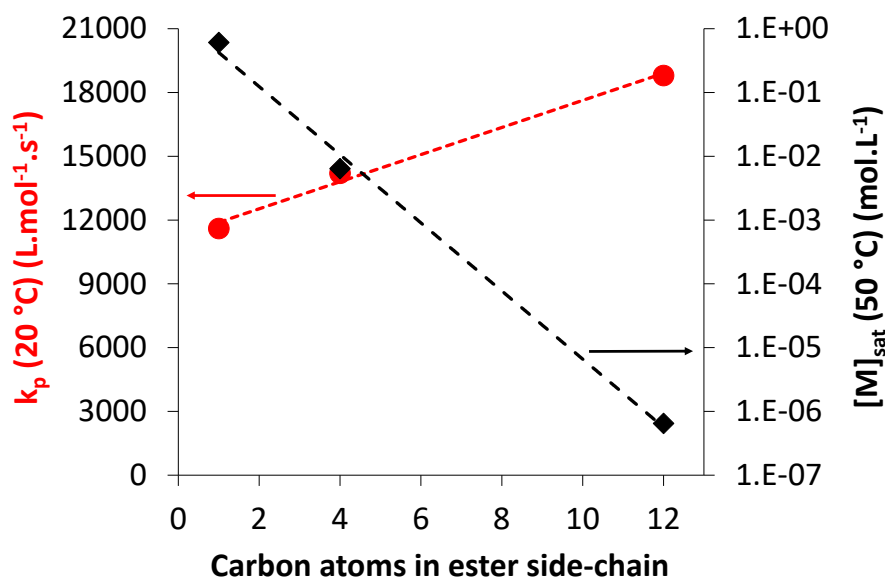


Figure S 16. (●) Propagation rate coefficients,  $k_p$ , reported for bulk homopolymerizations of  $n$ -alkyl acrylates at 20 °C and ambient pressure<sup>6</sup> and (◆) saturation concentration in water ( $[M]_{sat}$ ) of  $n$ -alkyl acrylates in water at 50 °C,  $[M]_{sat}$ .<sup>7</sup> Dotted lines represent linear regressions.

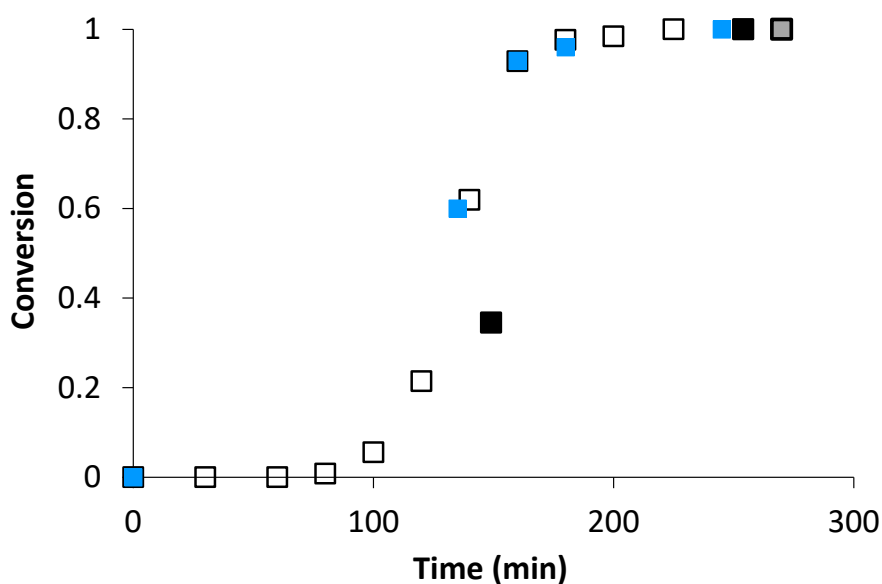


Figure S 17. Monomer conversion versus time for emulsion PISA at 70 °C of  $n$ BA polymerization mediated by PAA-TTC macroCTA, which was synthesized by RAFT polymerization carried out in either 1,4-dioxane (□ LBA-8 from PAA-TTC of 2700 g.mol<sup>-1</sup>, ■ LBA-9 from PAA-TTC of 5320 g.mol<sup>-1</sup>, ■ LBA-10 from PAA-TTC of 5320 g.mol<sup>-1</sup>) or in DMSO (■ LBA-12 from PAA-TTC of 3440 g.mol<sup>-1</sup>) (see Table S 6).



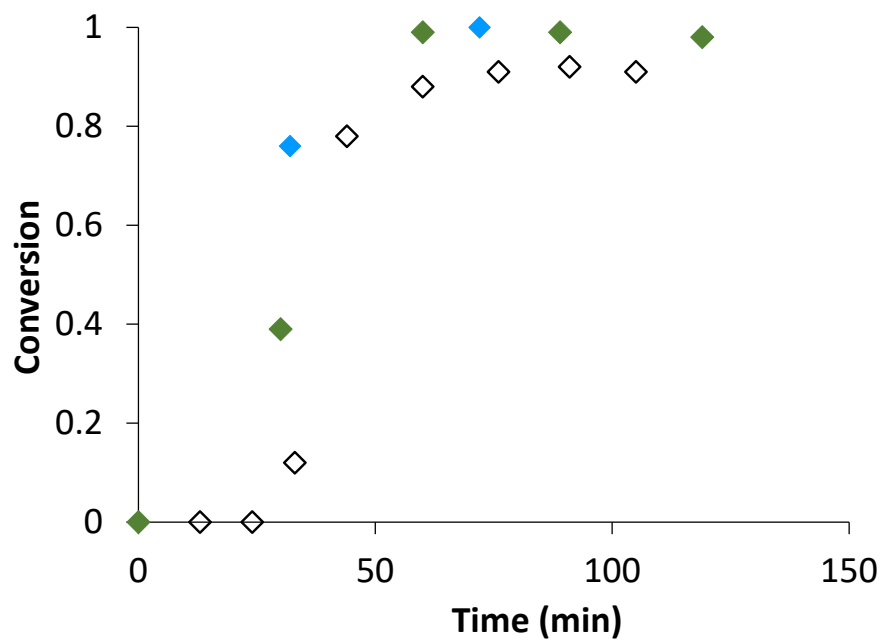


Figure S 18. Monomer conversion versus time for emulsion PISA at 70 °C of EA polymerization mediated by PAA-TTC macroCTA, which was synthesized by RAFT polymerization carried out in either 1,4-dioxane ( $\diamond$  LEA-14), or DMSO ( $\blacklozenge$  LEA-16) or DMF ( $\blacklozenge$  LEA-17) (see Table S 6).

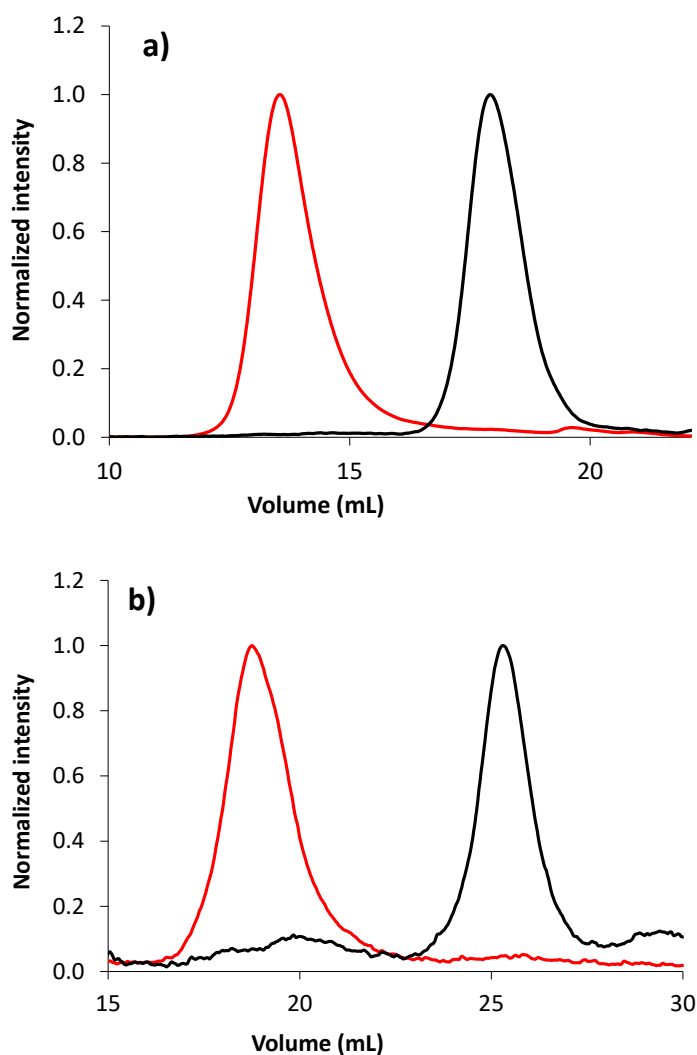


Figure S 19. Normalized refractometer traces of SEC chromatograms of (a) PAA-*b*-PnBA block copolymer (LBA-11 in Tables S7 and S8, set No. 1 of SEC columns) and (b) P(AA-*co*-EARB<sub>0.36%</sub>)-*b*-PnBA block copolymer (LBA-EARB3 in Table 2, set number No. 2 of SEC columns) synthesized by emulsion PISA. The black traces correspond to the first PAA-based macroCTA and the red traces to the diblock copolymer.

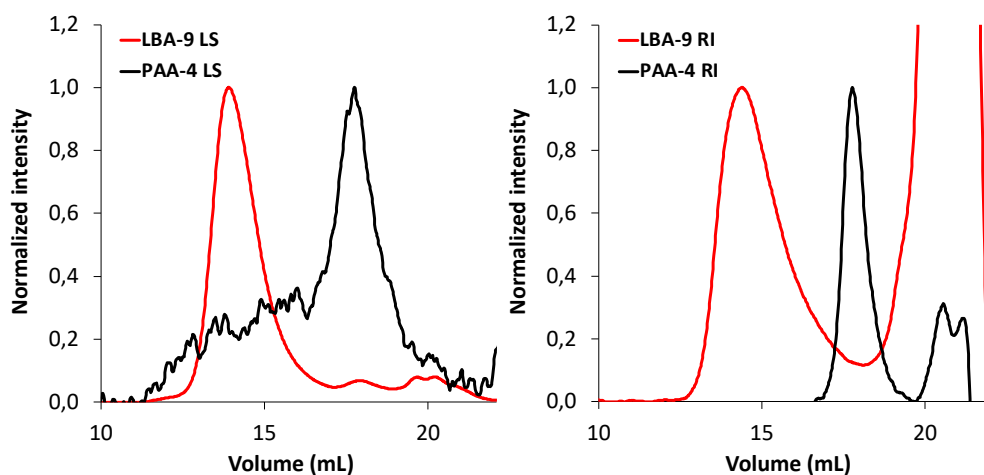


Figure S 20. Normalized SEC chromatograms (RI trace and LS trace at  $\theta = 90^\circ$ ) of PAA-*b*-PnBA block copolymers (LBA-9, Table S 6, Table S 7) synthesized by emulsion PISA (—) from PAA-TTC reactive stabilizers synthesized in 1,4-dioxane (—).

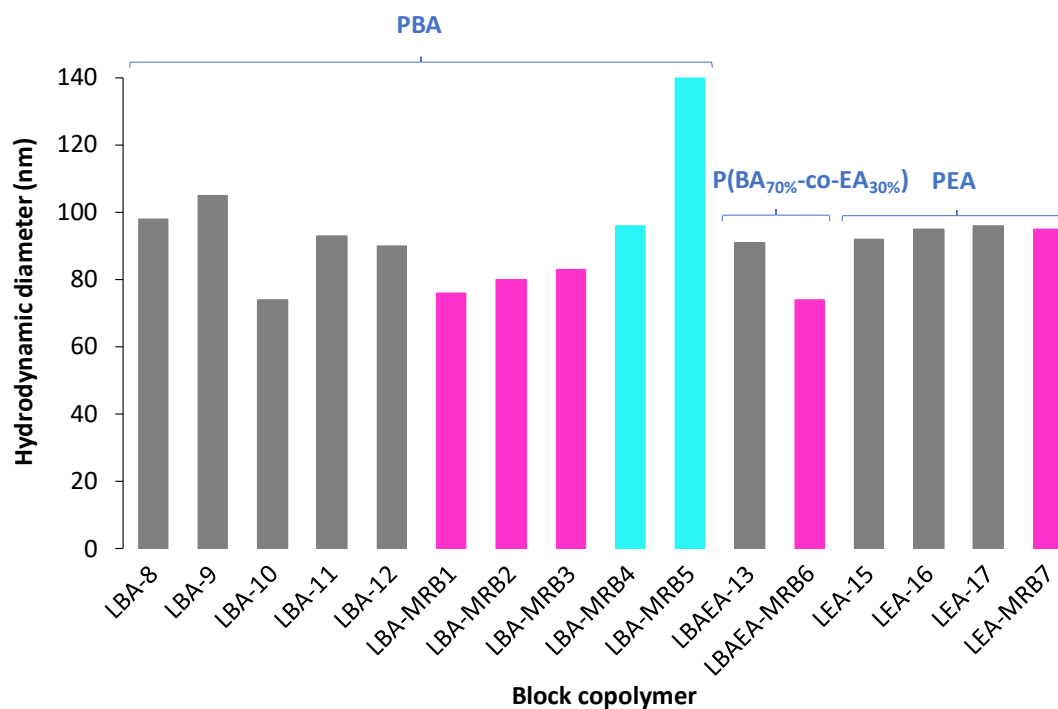


Figure S 21. Comparison of hydrodynamic diameters of block copolymers particles prepared from: ■ PAA-TTC, ■ P(AA-*co*-EARB)-TTC and ■ P(AA-*co*-VBRB)-TTC.

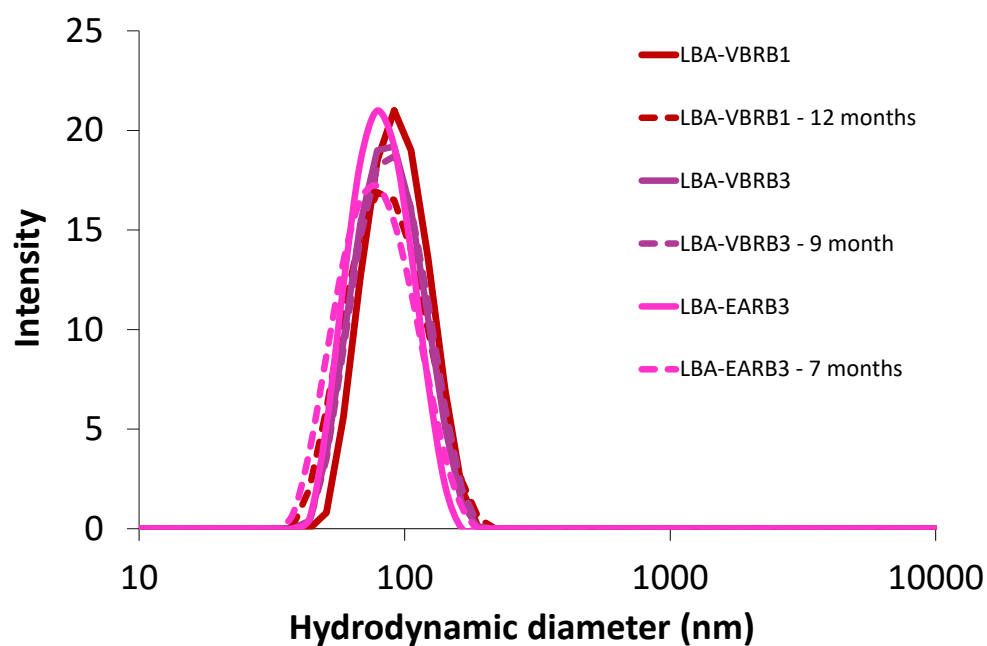
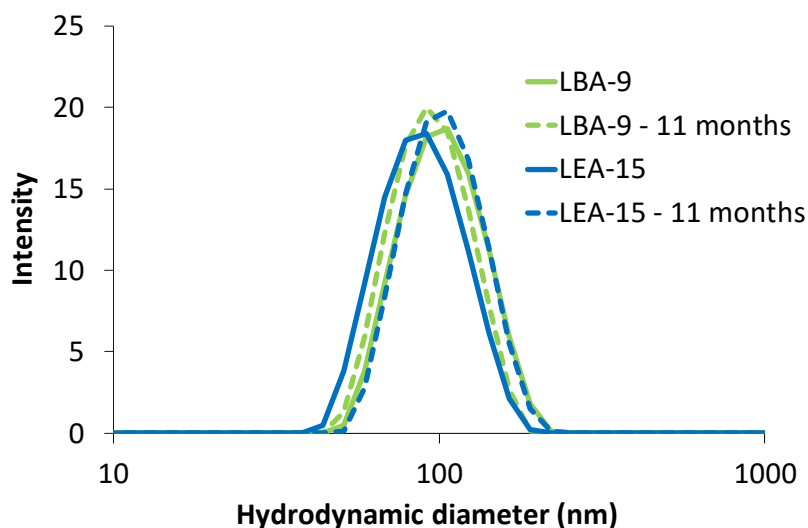


Figure S 22. Measurement of  $D_h$  of waterborne latexes in water over months. (Top) PAA-*b*-PnBA latexes: (— LBA-9, — LEA-15, see Table S7 †), (bottom) RB-based latex: — P(AA-*co*-VBRB<sub>0.1%</sub>)-*b*-PnBA (LBA-VBRB1), — P(AA-*co*-EARB<sub>0.36%</sub>)-*b*-PnBA (LBA-EARB3) and — PAA-*b*-P(nBA-*co*-VBRB<sub>0.1%</sub>) (LBA-VBRB3) (see Table 2 and Table 3 of article). DLS measurements performed at [Polymer] = 0.05 g.L<sup>-1</sup>.

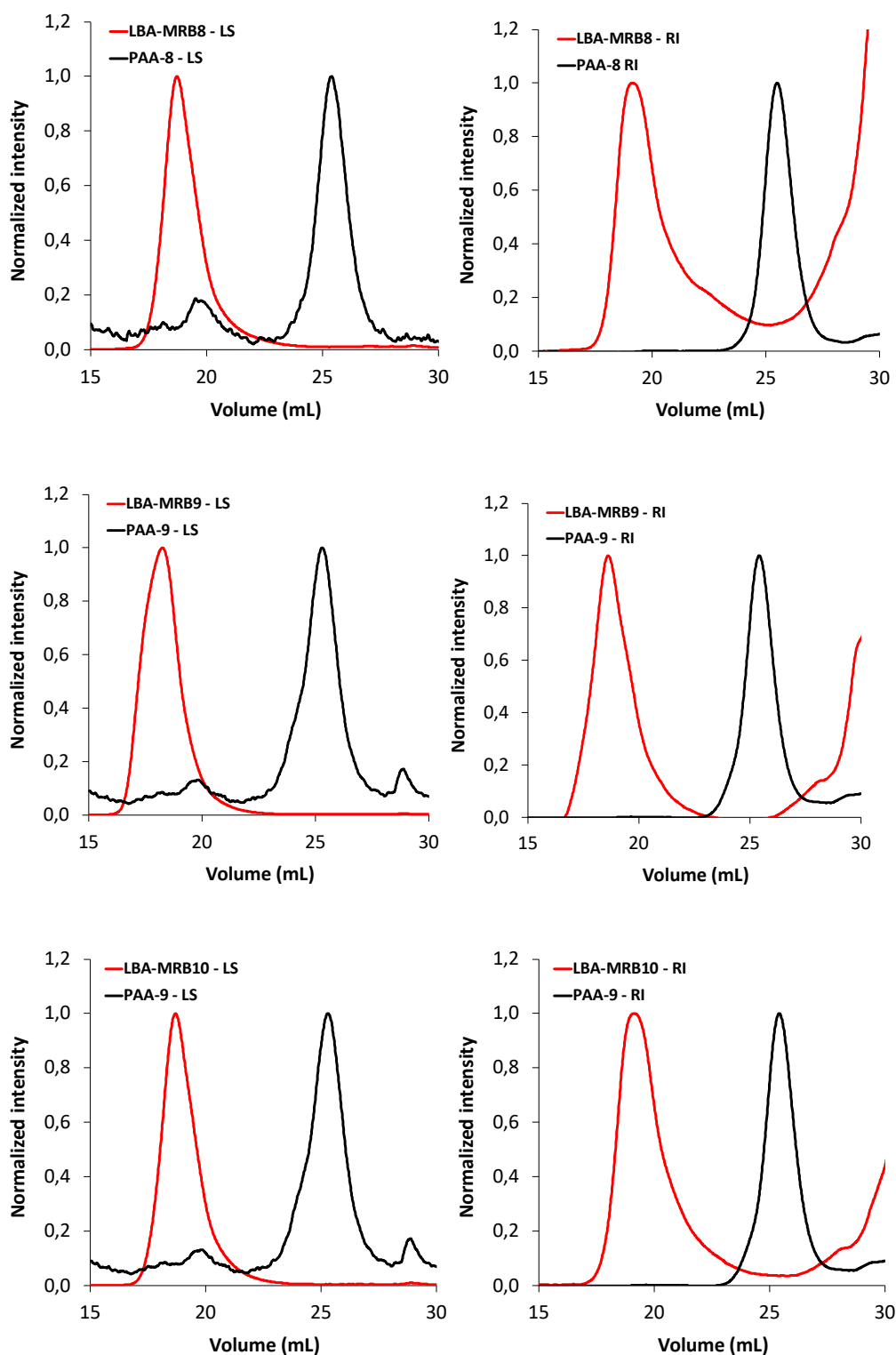


Figure S 23. Normalized SEC traces of block copolymers synthesized by emulsion PISA (**red** traces) from PAA-based macromolecular reactive stabilizers (**black** traces, PAA-TTC (PAA-8 and PAA-9)). From top to bottom: PAA-*b*-P(*n*BA-*co*-VBRB<sub>0.1%</sub>) (LBA-VBRB3), PAA-*b*-P(*n*BA-*co*-EARB<sub>0.1%</sub>) (LBA-EARB4), PAA-*b*-P(*n*BA-*co*-EARB<sub>0.1%</sub>) (LBA-EARB5). Both traces from refractometer (RI) and from MALLS detector (LS) are plotted. Set No.2 of SEC columns. See samples in Table 3 and Table S 1.

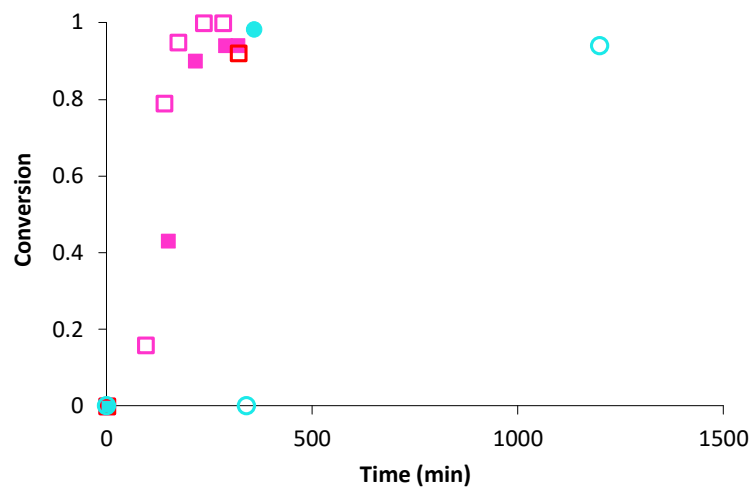


Figure S 24. *n*-butyl acrylate conversion versus time for synthesis of block copolymers by emulsion PISA: PAA-*b*-P(*n*BA-*co*-EARB<sub>0.1%</sub>) (□ LBA-EARB4 and □ LBA-EARB5) compared to P(AA-*co*-EARB<sub>0.1%</sub>)-*b*-P*n*BA (■ LBA-EARB1) and PAA-*b*-P(*n*BA-*co*-VBRB<sub>0.1%</sub>) (○ LBA-VBRB3) compared to P(AA-*co*-VBRB<sub>0.1%</sub>)-*b*-P*n*BA (● LBA-VBRB1).

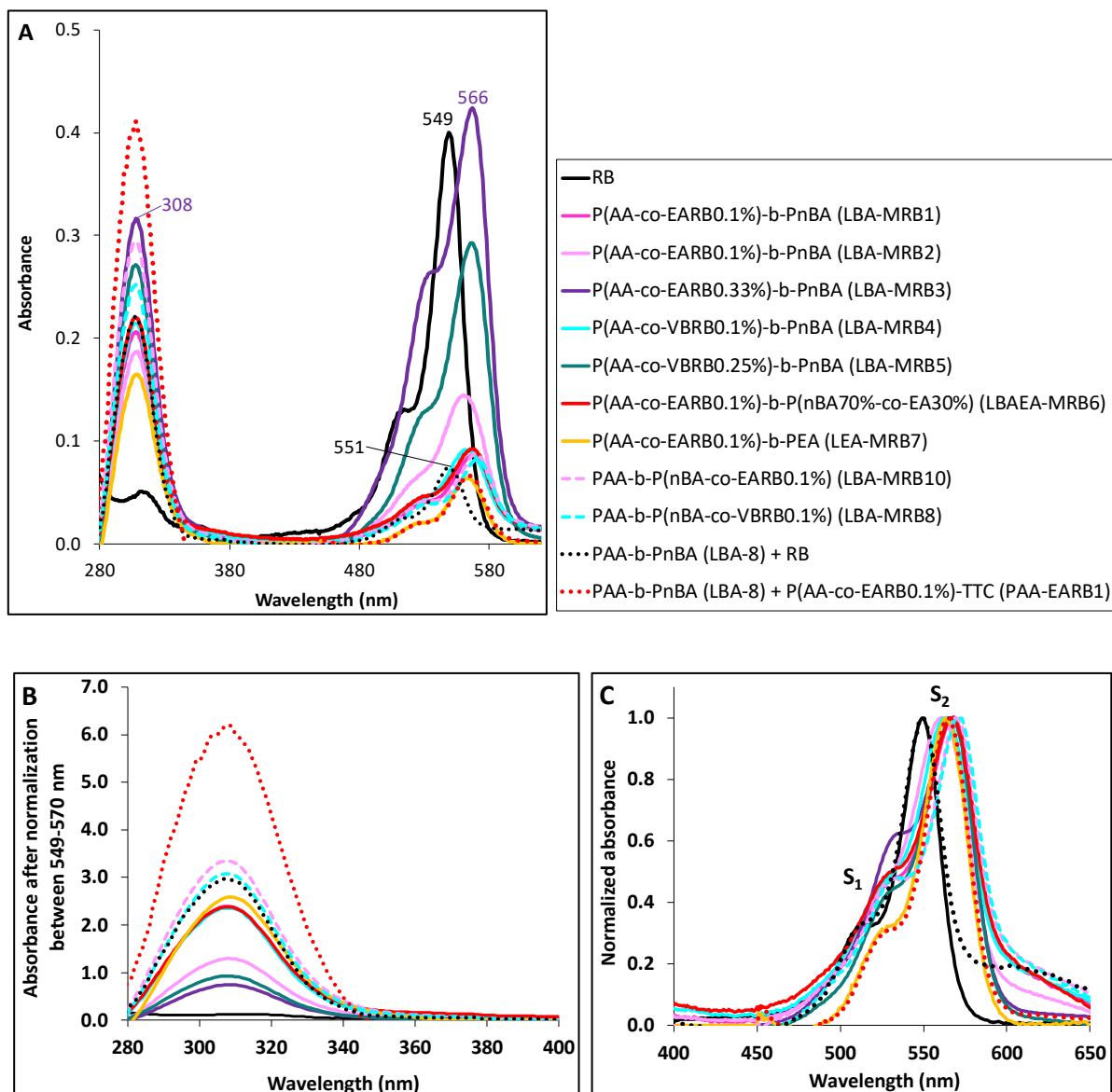


Figure S 25. A) Overlay of absorbance spectra of latexes at a polymer concentration of 2 g.L<sup>-1</sup> and of free RB (black plain line) in water; B) Overlay of normalized (at  $\lambda_{max}$  MRB) absorbance spectra of latexes and RB between 280 and 400 nm in water; C) Overlay of normalized (at  $\lambda_{max}$  MRB) absorbance spectra of latexes and RB between 400 and 650 nm after normalization at  $\lambda_{max}$  MRB.

Table S 8. Singlet oxygen quantum yield in water and RB loading of RB-based latexes.

Latex	Polymer	$\lambda_{\max}$ (RB/MRB) <sup>a</sup> (nm)	$S_2/S_1$ <sup>b</sup>	Theor. RB loading <sup>c</sup> ( $\mu\text{mol.g}^{-1}$ )	Exp. RB loading <sup>d</sup> ( $\mu\text{mol.g}^{-1}$ )	$\phi_{\Delta}(\text{H}_2\text{O})$ <sup>e</sup>
LBA-EARB1	P(AA-co-EARB <sub>0.1%</sub> )-b-PnBA	568	2.4	0.25	0.35	0.68 ± 0.07
LBA-EARB2	P(AA-co-EARB <sub>0.1%</sub> )-b-PnBA	560	2.4	0.51	0.63	0.73 ± 0.07
LBA-EARB3	P(AA-co-EARB <sub>0.36%</sub> )-b-PnBA	567	1.9	1.55	1.80	0.70 ± 0.07
LBA-VBRB1	P(AA-co-VBRB <sub>0.1%</sub> )-b-PnBA	562	2.2	0.34	0.36	0.57 ± 0.06
LBA-VBRB2	P(AA-co-VBRB <sub>0.25%</sub> )-b-PnBA	567	2.5	1.44	1.30	0.61 ± 0.06
LBAEA-EARB1	P(AA-co-EARB <sub>0.1%</sub> )-b-P(nBA <sub>70%</sub> -co-EA <sub>30%</sub> )	568	2.2	0.36	0.41	0.41 ± 0.04
LEA-EARB1	P(AA-co-EARB <sub>0.1%</sub> )-b-PEA	563	3.1	0.41	0.39	0.63 ± 0.06
LBA-EARB5	PAA-b-P(nBA-co-EARB <sub>0.1%</sub> )	570	2.6	0.53	0.36	0.74 ± 0.07
LBA-VBRB3	PAA-b-P(nBA-co-VBRB <sub>0.1%</sub> )	571	2.4	0.46	0.32	0.69 ± 0.07
LBA-8 + free RB	PAA-b-PnBA + free RB	548	3.0	0.39	0.39	0.74 ± 0.07
LBA-8 + PAA-EARB1	PAA-b-PnBA + P(AA-co-EARB <sub>0.1%</sub> )-TTC	564	3.1	0.29	0.32	0.70 ± 0.07

<sup>a</sup> Wavelength at the maximum RB absorbance. <sup>b</sup>  $S_2/S_1$  ratio determined from absorbance spectra of Figure S 25 at  $C_{\text{polymer}} = 2 \text{ g.L}^{-1}$ . <sup>c</sup> Theoretical RB loading (in  $\mu\text{mol}$  of MRB per gram of block copolymer) calculated by either Eq S. 8 for P(AA-co-MRB)-b-Poly(alkyl acrylate) or Eq S. 9 for PAA-b-P(nBA-co-MRB<sub>0.1%</sub>) copolymer. <sup>d</sup> Experimental RB loading (in  $\mu\text{mol}$  of MRB per gram of block copolymer) calculated from  $\lambda_{\max}$  (Eq S. 10). <sup>e</sup> Quantum yield of singlet oxygen production of latexes, determined by indirect method in water using furfuryl alcohol as quencher (see experimental part of article and part for determination of quantum yield in Supporting Information).

$$\text{Theor. RB loading}_{\text{copo}} (\mu\text{mol.g}_{\text{polymer}}^{-1}) = \frac{\text{Exp. RB loading}_{\text{macroCTA}} \times m_{\text{macroCTA}}}{m_{\text{macroCTA}} + (m_{\text{monomer}} \times \text{conversion})} \quad \text{Eq S. 8}$$



$$\text{Theor. RB loading}_{c_{\text{copo}}} (\mu\text{mol. g}_{\text{polymer}}^{-1}) = \frac{n_{\text{MRB},0}}{m_{\text{macroCTA}} + (m_{\text{monomer}} \times \text{conversion})} \quad \text{Eq S. 9}$$

$$\text{Exp. loading}_{c_{\text{copo}}} (\text{mol. g}_{\text{polymer}}^{-1}) = \frac{C_{\text{MRB}} \times V_{\text{cuvette}}}{m_{\text{copo}}} \quad \text{Eq S. 10}$$

The concentration  $C_{\text{MRB}}$  of MRB was determined from the absorbance at 559 nm through the Beer-Lambert law (

Eq S. 11), assuming that the molar extinction coefficient of MRB was the same as that of RB in water

since MRB monomers are insoluble in water.

$$A_{559 \text{ nm}} = \varepsilon_{\text{RB}} C_{\text{MRB}} l \quad \text{Eq S. 11}$$

with  $A_{559 \text{ nm}}$  the absorbance,  $\varepsilon_{\text{RB}}$  the molar extinction coefficient of RB in water ( $\varepsilon_{\text{RB } 549 \text{ nm, water}} = 113\,598 \text{ L.mol}^{-1}.\text{cm}^{-1}$ ) and  $l$  the path length ( $l = 1 \text{ cm}$ ).

Table S 9. Experimental values of  $T_g$  of PnBA, PEA and P( $nBA_{70\%}$ - $co$ -EA $_{30\%}$ ) of the hydrophobic block of copolymers synthesized.

Expt.	Block copolymer	$T_g$ of hydrophobic block (°C)
LBA-8	PAA- <i>b</i> -PnBA	-45
LEA-15	PAA- <i>b</i> -PEA	-12
LBA-EARB2	P(AA- <i>co</i> -EARB $_{0.1\%}$ )- <i>b</i> -PnBA	-44
LEA-EARB1	P(AA- <i>co</i> -EARB $_{0.1\%}$ )- <i>b</i> -PEA	-15
		-12
LBAEA-EARB1	P(AA- <i>co</i> -EARB $_{0.1\%}$ )- <i>b</i> - P( $nBA_{70\%}$ - $co$ -EA $_{30\%}$ )	-38

### Characterization of macromolecular features of polymers

i) Calculation of number-average molar mass ( $M_n$ ) of PAA-based macroCTA calculated from the experimental molar mass of the methylated samples obtained by SEC:

Molar masses of PAA-based macroCTA are calculated from the experimental molar mass of the methylated samples (*ie* poly(methyl acrylate), see Eq S. 12.

$$M_{n,PAA-TTC}(g \cdot mol^{-1}) = \frac{M_{n,PMA-TTC} - M_{TTC}}{M_{MA}} \times M_{AA} + M_{TTC} \quad \text{Eq S. 12}$$

With  $M_{TTC}$ ,  $M_{MA}$  and  $M_{AA}$  the molar masses of the molecular chain transfer agent, of methyl acrylate and acrylic acid monomers. This equation holds true for RB-based macroCTA.

$M_n$  of PAA-*b*-PnBA diblock copolymers were calculated from Eq S. 13.

$$M_{n,PAA-b-PnBA}(g \cdot mol^{-1}) = M_{n,PMA-b-PnBA} - M_{n,PMA-TTC} + M_{n,PAA-TTC} \quad \text{Eq S. 13}$$

With  $M_{n,PMA-b-PnBA}$  and  $M_{n,PMA-TTC}$  the molar masses of PMA-*b*-PnBA and PMA-TTC, respectively, provided by SEC. A similar equation is adapted for PAA-*b*-PEA and RB-based

block copolymers. Note that the methylation step can induce chain cleavage if the PAA is suspected to be branched.<sup>8</sup>

(ii) Error between molar mass of polystyrene standards and poly(alkyl acrylate) based on Mark-Houwink parameters:

Two polymers eluted at identical elution volumes, meaning that they have the same hydrodynamic volume, follows

Eq S. 14 :

$$[\eta]_1 M_1 = [\eta]_2 M_2 \quad \text{Eq S. 14}$$

With  $[\eta]$  the intrinsic viscosity and  $M$  the molar mass of polymers 1 and 2.

According to the MHS relation (

Eq S. 15) and MHS parameters, the molar mass of a polymer can be calculated

from a known molar mass of the first polymer according to

Eq S. 16.

$$[\eta] = KM^\alpha \quad \text{Eq S. 15}$$

$$\ln(M_2) = \frac{1}{1+\alpha_2} \times \ln\left(\frac{K_1}{K_2}\right) + \frac{1+\alpha_1}{1+\alpha_2} \times \ln(M_1) \quad \text{Eq S. 16}$$

$K$  and  $\alpha$  are the parameters of MHS. They are reported in Table S 10 for PS, PnBA and PEA.

Table S 10. Mark-Houwink Sakurada parameters of PS, PnBA and PEA homopolymers in THF at 30 °C.

Polymer	PS	PnBA	PEA
Reference	9	10	11
$\alpha$	0.716	0.700	0.774
$K$ (mL.g <sup>-1</sup> )	0.0114	0.0122	0.0057

The error between the molar mass extracted from a polystyrene calibration and the calculated mass of the poly(alkyl acrylate) is less than 10 % (Table S 11), with the hypothesis of absence of long chain branching.

Table S 11. Molar masses of PnBA and PEA calculated from PS calibration and MHS parameters.

Polymer 1 (standard)	M <sub>polymer 1</sub> (g.mol <sup>-1</sup> )	Polymer 2	M <sub>polymer 1</sub> (g.mol <sup>-1</sup> )	Error (%)
PS	150 000	PnBA	161 200	7.5
PS	150 000	PEA	150 500	0.3

(iii) Refractive index increments (dn/dc) of polymers for SEC-MALLS analysis:

The refractive index increments (dn/dc) of the PMA-*b*-PnBA, P(MA-*co*-MRB)-*b*-PnBA and PMA-*b*-P(*n*BA-*co*-MRB) diblock copolymers were determined using

Eq S. 17. This equation holds true for PEA-based block copolymers. The refractive index increments of the PMA-*b*-P(*n*BA<sub>70%-*co*</sub>-EA<sub>30%</sub>) and P(MA-*co*-MRB)-*b*-P(*n*BA<sub>70%-*co*</sub>-EA<sub>30%</sub>) diblock copolymers were determined using

Eq S. 18 .

$$\left(\frac{dn}{dc}\right)_{\text{copo}} = \omega_{\text{PAA}} \times \left(\frac{dn}{dc}\right)_{\text{PMA}} + \omega_{\text{PnBA}} \times \left(\frac{dn}{dc}\right)_{\text{PnBA}} \quad \text{Eq S. 17}$$

$$\left(\frac{dn}{dc}\right)_{\text{copo}} = \omega_{\text{PAA}} \times \left(\frac{dn}{dc}\right)_{\text{PMA}} + \omega_{\text{nBA}} \times \left(\frac{dn}{dc}\right)_{\text{PnBA}} + \omega_{\text{EA}} \times \left(\frac{dn}{dc}\right)_{\text{PEA}} \quad \text{Eq S. 18}$$

With  $\omega$  the weight fraction in the copolymer.

The dn/dc value of PMA was determined by analyzing five solutions of PMA in THF at different concentrations, ranging from 1 to 5 g.L<sup>-1</sup>. The peak area provided by the refractive index (RI) detector was plotted as a function of the polymer concentration (Figure S 26) and dn/dc was calculated from

Eq S. 19.

$$\text{Slope (mV. g}^{-1}\text{)} = \frac{\Delta \text{RI area}}{\Delta \text{Concentration}} = \frac{\text{RI Cal}}{n_0(\text{THF})} \times \frac{dn}{dc} \times V_{inj} \quad \text{Eq S. 19}$$

With *RI Cal* the calibration constant of the RI detector ( $6.355 \times 10^5 \text{ mV}\cdot\text{mL}^{-2}$ ),  $n_0$  (THF) the refractive index of THF (1.402) and  $V_{inj}$  the injected volume (0.1 mL).

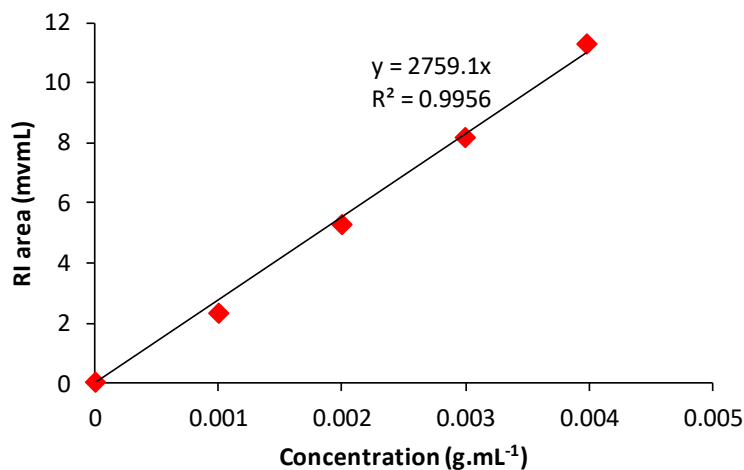


Figure S 26. RI peak area in SEC THF versus concentration for poly(methyl acrylate) PMA.

A value of  $dn/dc$  of  $0.061 \text{ mL}\cdot\text{g}^{-1}$  was found, in good agreement with the literature since Haddleton *et al.*<sup>12</sup> reported a  $dn/dc$  value of  $0.048 \text{ mL}\cdot\text{g}^{-1}$  for PMA in THF at ambient temperature and Loo *et al.* found a value of  $0.0548 \text{ mL}\cdot\text{g}^{-1}$  for PMA in THF at  $40 \text{ }^\circ\text{C}$ .<sup>13</sup> The value of  $dn/dc$  of PnBA and PEA homopolymers were taken from literature:  $(dn/dc)_{PnBA} = 0.065 \text{ mL}\cdot\text{g}^{-1}$  (reference<sup>14</sup>) and  $(dn/dc)_{PEA} = 0.073 \text{ mL}\cdot\text{g}^{-1}$  (reference<sup>11</sup>).

(iv) Equation for theoretical number-average molar mass

Theoretical number-average molar mass ( $M_{n,th}$ ) of PAA-based macroCTA was calculated from

Eq S. 20.

$$M_{n,th} \text{ (g}\cdot\text{mol}^{-1}\text{)} = M_{TTC} + \frac{[AA]_0}{[TTC]_0 + [ACPA]_0(1 - e^{-k_d t})} \times conversion \times M_{AA} \quad \text{Eq S. 20}$$

Here  $M_{TTC}$  corresponds to the molar mass of the molecular trithiocarbonate agent ( $M_{TTC} = 404 \text{ g}\cdot\text{mol}^{-1}$ ) and  $M_{AA}$  to the molar mass of acrylic acid ( $M_{AA} = 72 \text{ g}\cdot\text{mol}^{-1}$ ).  $[AA]_0$ ,  $[TTC]_0$  and  $[ACPA]_0$  are respectively the initial concentrations (in  $\text{mol}\cdot\text{L}^{-1}$ ) of the monomer, the chain

transfer agent and the initiator.  $k_d$  is the ACPA dissociation constant in 1,4-dioxane at 80 °C ( $k_d = 7.7 \times 10^{-5} \text{ s}^{-1}$ )<sup>14</sup> and  $t$  the polymerization time.

Theoretical  $M_n$  of PAA-*b*-P*n*BA copolymers, calculated from  
Eq S. 21.

$$M_{n,th} (g. mol^{-1}) = M_{PAA-TTC} + \frac{[nBA]_0 \times M_{nBA} \times Conversion}{[PAA-TTC]_0} \quad \text{Eq S. 21}$$

$M_{PAA-TTC}$  and  $M_{nBA}$  correspond respectively to the molar masses of the macromolecular chain transfer agent and of *n*BA monomer.  $[nBA]_0$  and  $[PAA-TTC]_0$  are the initial concentrations of *n*BA and macroCTA, respectively. The equation was adapted for EA homopolymerization with  $M_{EA}$ .

Theoretical number-average molar masses  $M_n$  of the PAA-*b*-P(*n*BA-*co*-EA) copolymers synthesized from an initial mixture of *n*BA and EA of 70/30 mol/mol were calculated from  
Eq S. 22.

$$M_{n,theo} (g. mol^{-1}) = M_{PAA-TTC} + \frac{([nBA]_0 \times M_{nBA} + [EA]_0 \times M_{EA}) \times Conversion}{[PAA-TTC]_0} \quad \text{Eq S. 22}$$

$M_{PAA-TTC}$ ,  $M_{nBA}$  and  $M_{EA}$  correspond to the molar masses of the macroCTA, *n*BA and EA monomers, respectively.

### ***UV-visible analyses of latexes***

The spectra of latexes in water were distorted because of the scattering properties of the latexes. Rayleigh scattering is a process in which electromagnetic radiation (including light) is scattered by a small spherical volume of variant refractive indexes, such as a particle, bubble, droplet, In order for Rayleigh's model to apply, the sphere must be much smaller in diameter than the wavelength ( $\lambda$ ) of the scattered wave. Typically, the upper limit is taken to be about 1/10 the

wavelength. In this size regime, the exact shape of the scattering center is usually not very significant and can often be treated as a sphere of equivalent volume. The degree of scattering varies as a function of the ratio of the particle diameter to the wavelength of the radiation, along with many other factors including polarization, angle, and coherence. The shorter blue wavelengths are more strongly scattered than the longer red wavelengths according to Rayleigh's  $1/\lambda^4$  relation. Considering the size of the latex particles (about 90 nm), the scattering effect was obviously observed between 850 and 300 nm, and was more pronounced at shorter wavelength. Accordingly, for the latex particles, the baseline deviation due to light scattering was corrected by a polynomial fit (Figure S 27).

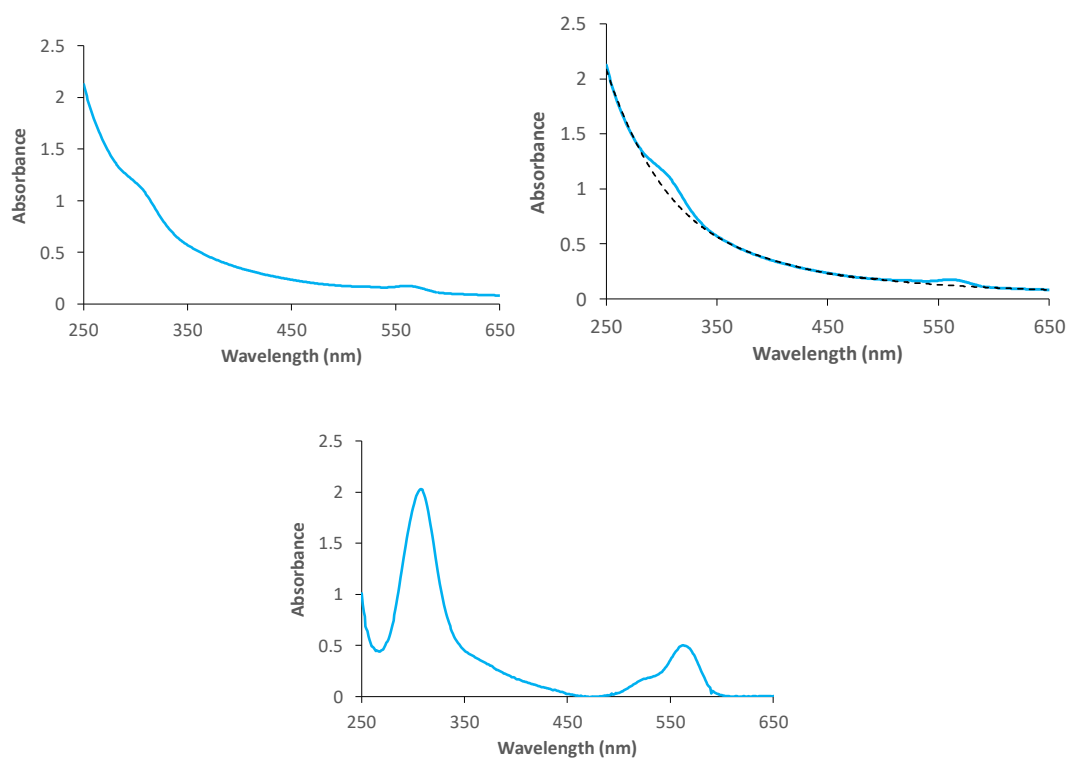


Figure S 27. (Top left) Raw data for absorbance versus wavelength of P(AA-co-VBRB<sub>0.1%</sub>)-*b*-PnBA latex (LBA-VBRB1) in water. (Top right) Example of polynomial fitting of the curve to set a baseline for subtraction of diffusion effects. (Bottom) Corrected spectrum of P(AA-co-VBRB<sub>0.1%</sub>)-*b*-PnBA latex (LBA-VBRB1) in water.

It was controlled that with such a correction, the experimental loading of a RB-free latex PAA-*b*-PBA (LBA-8) to which a controlled mass of free RB was added was the correct value (Figure S 28). In this latter case, the baseline polynomial correction was

$$y = 1,4384E-15x^6 - 5,1305E-12x^5 + 7,5625E-09x^4 - 5,9099E-06x^3 + 2,5934E-03x^2 - 6,1073E-01x + 6,1239E+01 \quad (R^2 = 0,9999).$$

The calculated RB concentration was  $6.43 \cdot 10^{-7}$  M from the diffusion-corrected spectrum for  $6.38 \cdot 10^{-7}$  M introduced in the cuvette.

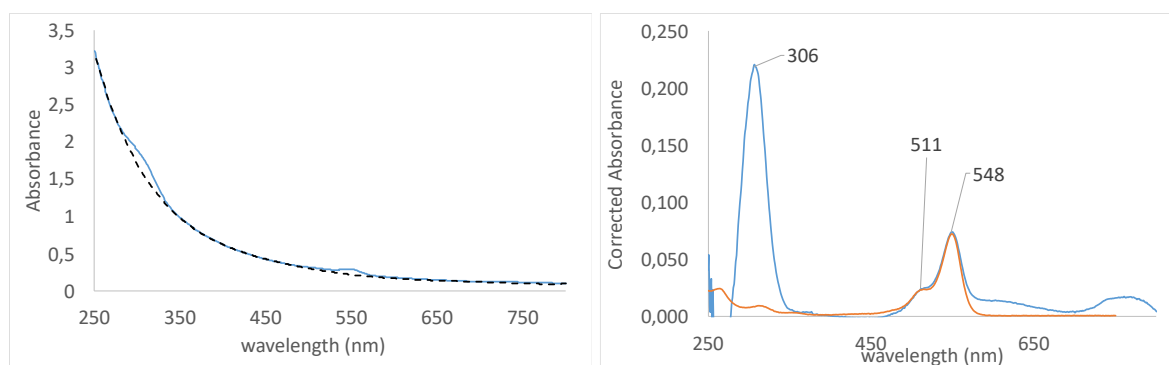


Figure S 28. Left, Blue: Raw spectrum of PAA-*b*-PBA (LBA-8) + Free RB ( $6.38 \cdot 10^{-7}$  M in water); Left, Dotted black line: Polynomial fitting of the curve to set the baseline. Right, Blue: Corrected spectrum for scattering of PAA-*b*-PBA (LBA-8) + Free RB; Right, Orange: Theoretical spectrum of RB at  $6.38 \cdot 10^{-7}$  M in water deduced from its molar absorption coefficient.

### ***Monitoring of the singlet oxygen production***

The rate of disappearance of the quencher  $Q$  (here furfuryl alcohol or FFA) at the very beginning of the reaction (less than 10 % variation of  $[Q]$ ) with singlet oxygen ( $r_{ox}$ ) is given by Eq S. 23. <sup>1</sup>

$$r_{ox} = -\frac{d[Q]}{dt} = P_a^{Sens} \phi_{\Delta}^{Sens} \frac{k_r^Q [Q]}{k_d + k_t^Q [Q]} \quad \text{Eq S. 23}$$

with  $k_r^Q = 7 \times 10^7$  L.mol<sup>-1</sup>.s<sup>-1</sup>, rate constant of chemical quenching of FFA by <sup>1</sup>O<sub>2</sub>

and  $k_t^Q = 1.2 \times 10^8$  L.mol<sup>-1</sup>.s<sup>-1</sup> rate constant of singlet oxygen <sup>1</sup>O<sub>2</sub> total quenching by FFA.

$k_d = 3.03 \times 10^5$  s<sup>-1</sup>, rate constant of the non-radiative decay of singlet oxygen in water

$\phi_{\Delta}^{Sens}$  quantum yield of singlet oxygen production by the sensitizer under investigation



$P_a^{Sens}$  (Einstein.L<sup>-1</sup>.s<sup>-1</sup>) is the photon flux absorbed by the sensitizer at the wavelength of excitation. According to the Beer-Lambert law,  $P_a^{Sens}$  depends on the absorbance of the sensitizer at the excitation wavelength ( $A_{Sens}$ ) and on the incident photon flux  $P_0$  (Einstein.L<sup>-1</sup>.s<sup>-1</sup>) (Eq S. 24).  $P_a^{Sens}$  is represented by the grey part Figure S 29 corresponding to the overlap between the irradiance spectrum of the LED ( $P_0$ ) and the absorbance spectrum of the photosensitizer ( $A_{Sens}$ ).

$$P_a^{Sens} = P_0(1 - 10^{-A_{Sens}}) \quad \text{Eq S. 24}$$

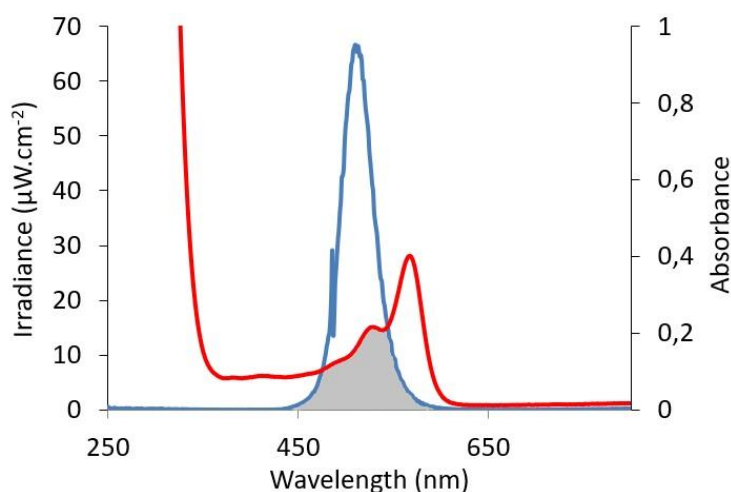


Figure S 29. Overlay of the irradiance spectrum of the LED and the absorbance spectrum of a RB-based material.

Under our conditions the term  $k_t^Q[Q]$  is less than 10% of  $k_d$ . Accordingly, the first-order analysis of the reaction rate holds true (Eq S. 25).

$$\ln\left(\frac{[Q]}{[Q_0]}\right) = -P_a^{Sens} \phi_{\Delta}^{Sens} \frac{k_r^Q}{k_d} t \quad \text{Eq S. 25}$$

$\phi_{\Delta}^{Sens}$  may also be determined in comparative experiments according to Eq S. 26 after controlling that, under our conditions,  $\phi_{\Delta}^{RB}$  of the reference sensitizer Rose Bengal in water was consistent with the literature value ( $\phi_{\Delta}^{RB}=0.76$  in water)<sup>15</sup>:

$$\phi_{\Delta}^{Sens} = \phi_{\Delta}^{RB} \frac{P_a^{RB} r_{ox}^{Sens}}{P_a^{Sens} r_{ox}^{RB}} \quad \text{Eq S. 26}$$

This method implies several measurements: the absorbance spectrum of the photosensitizing material, the irradiance of the light source and the variation of the concentration of the quencher. An error of 10% can be estimated when adding all the uncertainties of these measurements.

The reaction of furfuryl alcohol with singlet oxygen is described in Figure S 30. The degradation of FFA was analyzed by high performance liquid chromatography (HPLC) and not by UV-vis spectroscopy because the absorbance spectra of FFA and its degradation product (pyranone) overlapped.

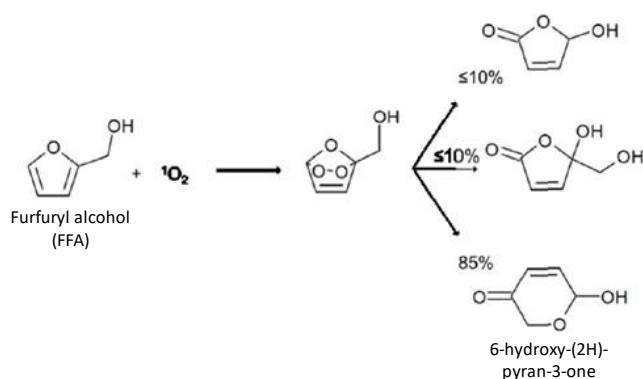


Figure S 30. Photo-oxygenation of furfuryl alcohol by in situ produced singlet oxygen

Several 3 mL samples of a mixture of latex (concentration ranging between  $1 \times 10^{-7}$  M and  $5 \times 10^{-7}$  M for an absorbance of the solution ranging from 0,01 to 0,1) and FFA (concentration  $1.0 \times 10^{-4}$  M, prepared from a stock solution of freshly distilled FFA) in milliQ water were prepared and consecutively introduced in the irradiation cuvette installed in the optical bench (Figure S 31 left). With each sample the light source was lighted on during variable time intervals (typically 0, 1, 2, 5, 10, 15 and 30 min). The light source was a high-power LED (Roithner LaserTechnik) with 515 nm emission wavelength. Its emission spectrum was measured before the irradiation experiments with the spectroradiometer detector exactly at the same position as

the sample cuvette. The spectroradiometer was an Avaspec 2048L equipped with a  $1\text{ m} \times 600\text{ }\mu\text{m}$  UV optic fiber and a  $3900\text{ }\mu\text{m}$   $180^\circ$  cosin corrector. The irradiated window from the LED was  $1.18\text{ cm}^2$  in the 3 mL cuvette but the irradiation was assumed to be spread in the whole 3 mL volume due to efficient stirring in the cuvette. Thus, the calculations were done considering the decrease of FFA concentrations in the 3 mL volume of the cuvette. After irradiation, the 3 mL samples were transferred into test tubes and kept in the dark up to the end of the experiment. For each irradiated sample, 1 mL was used for HPLC measurements, while the absorbance spectra of the remaining 2 mL samples were recorded to check the sensitizer stability. HPLC analysis was carried out with Agilent 1290 equipped with a Supelco Lichrosphere RP18-5 ( $25\text{ mm} \times 4.6\text{ mm}$ ,  $5\text{ }\mu\text{m}$ ) column,  $20\text{ }\mu\text{L}$  injection, eluent 80% water with 0,1%  $\text{H}_3\text{PO}_4$ , 20% acetonitrile, rate  $2\text{ mL}\cdot\text{min}^{-1}$ , UV detection at 205 nm and 218 nm. The retention times of FFA and 6-hydroxy-(2H)-pyran-3-one were 2.9 min and 1.8 min, respectively (Figure S 31, right). An external calibration was done with 5 dilutions of FFA to convert peak areas to concentrations.

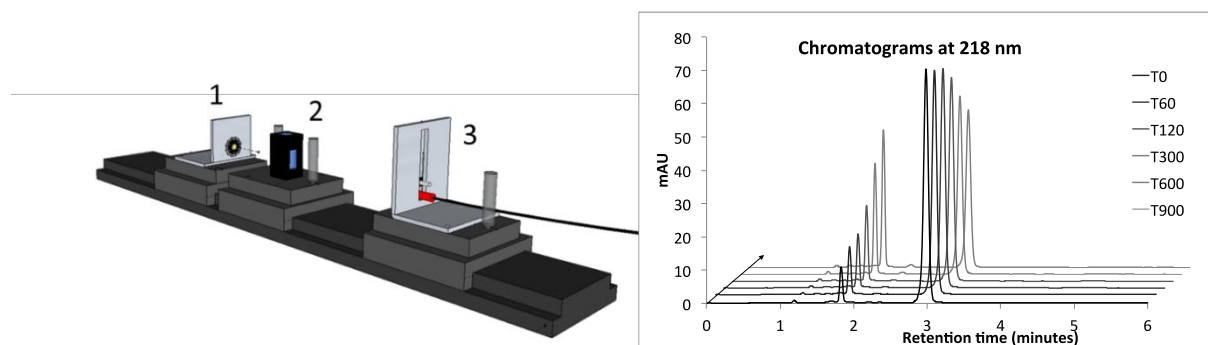


Figure S 31. Left) Scheme of the optical bench used for irradiation experiments (1: light source (LED), 2: cuvette holder, 3: holder for the spectroradiometer cell). Right) Example of HPLC-UV chromatogram.

### *Limit concentration of solubility of VBRB measured in solvents and monomers*

Table S 12. Average range of solubility of VBRB measured for the present work

Solvent or Monomer	[VBRB] <sub>max</sub> (mol L <sup>-1</sup> )
Dimethyl sulfoxide	0.30
1,4-Dioxane	0.20
Ethanol	0.05
Methyl acrylate	0.002
Ethyl acrylate	0.001
Butyl acrylate	0.0005

## References

- Petrizza, L.; Le Behec, M.; Decompte, E.; El Hadri, H.; Lacombe, S.; Save, M. Tuning Photosensitized Singlet Oxygen Production from Microgels Synthesized by Polymerization in Aqueous Dispersed Media. *Polymer Chemistry* **2019**, *10*, 3170-3179.
- Boussiron, C.; Le Behec, M.; Petrizza, L.; Sabalot, J.; Lacombe, S.; Save, M. Synthesis of Film-Forming Photoactive Latex Particles by Emulsion Polymerization-Induced Self-Assembly to Produce Singlet Oxygen. *Macromolecular Rapid Communications* **2019**, *40*.
- Maria Nowakowska; Mariusz Kepczynski; Szczubialka, K. New Polymeric Photosensitizers. *Pure Applied Chemistry* **2001**, *73*, 491-495.
- Reichardt, C. Solvatochromic Dyes as Solvent Polarity Indicators. *Chemical Reviews* **1994**, *94*, 2319-2358.
- Kamlet, M. J.; Abboud, J. L. M.; Abraham, M. H.; Taft, R. W. Linear Solvation Energy Relationships. 23. A Comprehensive Collection of the Solvatochromic Parameters, .Pi.\*, .Alpha., And .Beta., and Some Methods for Simplifying the Generalized Solvatochromic Equation. *The Journal of Organic Chemistry* **1983**, *48*, 2877-2887.
- Beuermann, S.; Buback, M. Rate Coefficients of Free-Radical Polymerization Deduced from Pulsed Laser Experiments. *Prog. Polym. Sci.* **2002**, *27*, 191-254.
- Herk, A. M. V. Chemistry and Technology of Emulsion Polymerization. *Blackwell Publishing* **2005**.
- Lacík, I.; Stach, M.; Kasák, P.; Semak, V.; Uhelská, L.; Chovancová, A.; Reinhold, G.; Kilz, P.; Delaittre, G.; Charleux, B.; Chaduc, I.; D'Agosto, F.; Lansalot, M.; Gaborieau, M.; Castignolles, P.; Gilbert, R. G.; Szablan, Z.; Barner-Kowollik, C.; Hesse, P.; Buback, M. Sec Analysis of Poly(Acrylic Acid) and Poly(Methacrylic Acid). *Macromolecular Chemistry and Physics* **2015**, *216*, 23-37.
- Hutchinson, R. A.; Paquet, D. A. J.; McMinn, J. H.; Beuermann, S.; Fuller, R. E.; Jackson, C. *Dechema Monographs* **1995**, *131*, 467.
- Beuermann, S.; Paquet, D. A.; McMinn, J. H.; Hutchinson, R. A. Determination of Free-Radical Propagation Rate Coefficients of Butyl, 2-Ethylhexyl, and Dodecyl Acrylates by Pulsed-Laser Polymerization. *Macromolecules* **1996**, *29*, 4206-4215.

11. Couvreur, L.; Piteau, G.; Castignolles, P.; Tonge, M.; Coutin, B.; Charleux, B.; Vairon, J.-P. Pulsed-Laser Radical Polymerization and Propagation Kinetic Parameters of Some Alkyl Acrylates. *Macromolecular Symposia* **2001**, *174*, 197-208.
12. Levere, M. E.; Willoughby, I.; O'Donohue, S.; de Cuendias, A.; Grice, A. J.; Fidge, C.; Becer, C. R.; Haddleton, D. M. Assessment of Set-Lrp in DmsO Using Online Monitoring and Rapid Gpc. *Polymer Chemistry* **2010**, *1*.
13. Guice, K. B.; Loo, Y.-L. Reversible Phase Transformations in Concentrated Aqueous Block Copolymer Solutions of Poly(Methyl Acrylate)-B-Poly(Hydroxyethyl Methacrylate-Co-Dimethylaminoethyl Methacrylate). *Macromolecules* **2007**, *40*, 9053-9058.
14. Brandrup, J.; Immergut, E. H.; Grulke, E. A. *Polymer Handbook 4th Edition* **2003**, John Wiley & Sons.
15. Wilkinson, F.; Helman, W. P.; Ross, A. B. Quantum Yields for the Photosensitized Formation of the Lowest Electronically Excited Singlet State of Molecular Oxygen in Solution. *Journal of Physical and Chemical Reference Data* **1993**, *22*, 113-262.